JMEPEG
https://doi.org/10.1007/s11665-025-12551-1

1059-9495/$19.00

ORIGINAL RESEARCH ARTICLE

Advanced Process Modeling and Optimization of Wire Electrical Discharge Machining for Austenitic Stainless Steel Using Statistical and Desirability Frameworks

R. Ashok Gandhi, VijayAnanth Suyamburajan, S. Sambath, and V. Jayaseelan

Submitted: 28 May 2025 / Revised: 13 October 2025 / Accepted: 17 October 2025

This study investigates the optimization of Wire EDM parameters for X5CrNi18-10 austenitic stainless steel, focusing on maximizing cutting rate (CR) while minimizing surface roughness (Ra) and cut width (CW). A response surface methodology based on a Box–Behnken Design was employed to conduct experiments and develop predictive models for the responses as a function of voltage (*V*), pulse interval (*I*), pulse duration (*D*), and cutting feed (*F*). ANOVA revealed that pulse duration and cutting feed significantly influenced all three responses. Pulse interval also showed significant effects on CR and CW. Quadratic regression models were developed, demonstrating a good fit for CR and CW, while the Ra model indicated a significant lack of fit. Multi-criteria optimization using the desirability framework identified an optimal parameter set (*V* = 65 volts, *I* = 45.49 μs, *D* = 103.57 μs, *F* = 8.94 m/min) achieving a high combined desirability of 0.903. A validation experiment at these settings yielded a CR of 41.73 mm^3/min, an Ra of 1.03 μm, and a CW of 0.315 mm, showing good agreement with predictions for CR and CW but a larger deviation for Ra. Surface morphology analysis using SEM revealed rougher surfaces at maximum CR conditions compared to the finer texture at optimized conditions. Surface roughness profiles confirmed a significant reduction in Ra at the optimized settings. Video measuring instrument images showed a narrower and more uniform cut at optimized conditions compared to the wider kerf at maximum CW conditions. The optimized parameters offer a balanced performance, and the developed models can be utilized for predicting and controlling the Wire EDM process for this material.

Keywords austenitic stainless steel, cut width, cutting rate, response surface methodology, surface roughness, wire EDM

1. Introduction

Wire Electrical Discharge Machining (Wire EDM) has emerged as an indispensable non-traditional machining technique, particularly suited for materials that are difficult to machine using conventional techniques (Ref 1). This spark erosion mechanism allows the machining of complex and high-precision components with minimal mechanical stress on the work material, rendering it a highly suitable approach for aerospace, medical, and tooling applications (Ref 2-4). Austenitic stainless steel (ASS), specifically X5CrNi18-10 (equivalent to AISI 304/SS304), represents one such material that is widely utilized due to its excellent formability, weldability, and corrosion resistance. It finds applications in cryogenic vessels, medical instruments, marine equipment, and nuclear reactors (Ref 5). The precision requirements and complexity associated with components made of SS304 make Wire EDM an essential technology for manufacturing such parts (Ref 6). Wire EDM provides clear advantages in creating intricate geometries, sharp corners, and components with tight tolerances without inducing mechanical deformation or thermal stress concentration zones. Its benefits are largely contingent upon the precise control and optimization of process parameters such as pulse-on time, pulse-off time, peak current, voltage, wire tension, and dielectric flow rate. These parameters significantly influence critical machining responses, including material removal rate (MRR), surface roughness, and kerf width (Ref 7, 8). The optimization of Wire EDM process parameters has been an area of active research. Vijayakumar and Chandradass (2024) emphasized that pulse-on and -off times, wire feed, and servo voltage play substantial roles in determining the quality of the machined surfaces. The Design of Experiments (DOE) technique is widely used to analyze parameter effects and derive optimal settings for specific outcomes such as higher MRR or lower surface roughness (Ref 9). Lingadurai et al. (2012) employed DOE on SS304 using brass wire electrodes and revealed that pulse-on time significantly affects kerf width, wire feed impacts surface roughness, and voltage primarily influences MRR (Ref 10). Gowd et al. (2014) conducted a study involving Response Surface Methodology (RSM) to establish predictive models and optimize the

R. Ashok Gandhi, Department of Mechanical Engineering, Sri Sai Ram Engineering College, Chennai 600044, India; **VijayAnanth Suyamburajan**, Department of Mechanical Engineering, VELS Institute of Science, Technology and Advanced Studies, Chennai 600117, India; **S. Sambath**, Department of Mechanical Engineering, SRM Madurai College for Engineering and Technology, Sivaganga 630612, India; and **V. Jayaseelan**, Department of Mechanical Engineering, Saveetha Engineering College, Chennai 602105, India. Contact e-mail: jaiseelanv@gmail.com.

Published online: 01 November 2025

machining parameters for MRR and surface roughness. These findings pointed out that multi-objective optimization using the Non-dominated Sorting Genetic Algorithm (NSGA) could yield a Pareto optimal front, balancing the trade-offs between competing objectives (Ref 11).

Azawqari et al. (2024) employed a Taguchi-based DOE and concluded that pulse-on time and current are dominant factors affecting both kerf and MRR, whereas pulse-off time also significantly impacts surface roughness. The use of utility-based optimization and Grey Relational Analysis (GRA) has also gained popularity in recent literature (Ref 12). Mathew et al. (2014) applied a utility concept for the multi-objective optimization of Wire EDM parameters and determined optimal combinations for pulse-on/off time, wire feed, tension, and dielectric pressure using an L27 orthogonal array and ANOVA (Ref 13). Similarly, Naeim et al. (2024) used a full factorial design and MATLAB image processing to quantify slot geometry, offering insights into the influence of traverse feed and current on MRR and pulse durations on surface roughness (Ref 14). Ishfaq et al. (2019) used a grey relational approach to address the stochastic nature of Wire EDM and highlighted the difficulty in achieving optimal topography on SS304 due to its high thermal resistance. This research demonstrated that current and voltage are the primary influencers for cutting speed and kerf, whereas surface roughness is majorly affected by voltage, drum speed, and nozzle offset (Ref 15). Rathod et al. (2025) conducted a study using RSM on SS304 workpieces and confirmed the effectiveness of this method in identifying optimal parameters for maximum MRR and minimum surface roughness (Ref 16). Seshaiah et al. (2022) demonstrated the relevance of pulse parameters and dielectric flow on machining performance, particularly focusing on the trade-off between surface finish and material removal efficiency (Ref 17). Chaudhary et al. (2019) explored the effect of wire tension on surface roughness, MRR, and surface microhardness while finding no significant impact on kerf width (Ref 18). Srinivasan et al. (2022) applied regression-based algorithms to predict MRR and surface roughness and found that multilayer perceptron models yielded high correlation coefficients (0.999 for MRR, 0.995 for surface roughness), thus demonstrating the efficacy of AI tools for predictive analytics in Wire EDM (Ref 19). Khan et al. (2014) confirmed that pulse duration is the most influential parameter for both surface roughness and kerf width using GRA and ANOVA, reiterating pulse duration's central role in surface finish quality (Ref 20). Natarajan et al. (2022) developed multiple regression models to empirically link process variables to outcomes in SS304 machining. This work highlighted the transition from trial-and-error to predictive modeling using Taguchi response analysis for optimizing pulse parameters (Ref 21). El-Bahloul (2020) compared RSM and Artificial Neural Networks (ANN) and concluded that a hybrid RSM-ANN approach, augmented with fuzzy logic, provides a robust tool for optimizing Wire EDM operations. This study affirmed that increasing pulse duration and input current improves MRR but deteriorates surface roughness, underscoring the ever-present trade-off in Wire EDM performance (Ref 22). In a recent comprehensive study, Saiyathibrahim et al. (2025) implemented GRA and Genetic Algorithm (GA) to optimize Wire EDM parameters for AISI 304, achieving a notable performance enhancement of 54.36% in machining outcomes. This work confirmed that optimizing pulse duration and interval, while minimizing applied voltage, yielded better MRR and surface roughness (Ref 23).

There is extensive research on the application of Wire EDM to austenitic stainless steels such as X5CrNi18-10 (AISI 304). However, a critical gap persists in the literature; most studies fail to adopt a statistically rigorous and integrated framework for the simultaneous optimization of key performance measures: Cutting Rate (CR), Surface Roughness (Ra), and Cut Width (CW). Instead, previous works often concentrate on one or two of these responses in isolation, overlooking the crucial trade-offs that exist between machining productivity, surface integrity, and dimensional precision. This lack of a unified approach limits the practical utility of the findings, especially in real-world manufacturing settings where multiple criteria must be optimized together. The novelty of the present study lies in its development of a holistic, multi-objective optimization strategy specifically tailored for Wire EDM of X5CrNi18-10 ASS. A key contribution is the integration of RSM (specifically the Box–Behnken Design) with a desirability function approach to determine a single, optimal parameter set that effectively balances the conflicting objectives of CR, Ra, and CW. The study offers a comprehensive parametric investigation, including both widely studied input factors such as voltage, pulse interval, and pulse duration and lesser-explored variables like cutting feed. The inclusion of cutting feed introduces a new dimension to the understanding of process behavior, especially in terms of its interaction with traditional parameters, thereby addressing a significant oversight in the existing literature. To ensure both statistical and practical relevance, the developed predictive models are thoroughly validated through statistical diagnostics and experimental confirmation.

2. Materials and Methods

2.1 Materials

The experiments were conducted using a rectangular specimen made of X5CrNi18-10 (AISI 304) austenitic stainless steel (ASS), measuring 100 mm by 150 mm with a thickness of 10 mm. This type of stainless steel is characterized by a density of 8.03 g/cm^3 and a tensile strength of 600 MPa. It has a specific heat capacity of 0.5 J/g °C and a hardness of 129 HV. The material's melting point is 1450 °C, and it possesses a thermal conductivity of 16.2 W/m K (Ref 18). Table 1 presents the spectrometric chemical composition of the material used in this study.

2.2 Experimental Procedure

Wire EDM was carried out using a CNC Electronica machine, with machining parameters determined through extensive preliminary testing. De-mineralized water was utilized as the dielectric fluid, while a 0.25 mm diameter brass wire functioned as the tool electrode. A constant wire tension of 8 N was maintained throughout all experiments. The procedural workflow followed in this study is illustrated in Fig. 1. Three primary performance metrics were investigated: Cutting Rate (CR), Surface Roughness (Ra), and Cut Width (CW). The cutting rate, expressed in mm^3/min, was calculated by measuring the mass of the workpiece before and after machining using a high-precision balance and converting this weight loss into volume removed over time. Surface roughness was measured after machining using a Surfcorder SE3500K profilometer, following standard industry practices. A cut-off length of

Table 1 Chemical composition (wt.%) of X5CrNi18-10 ASS

Element	Ni	Mn	Cr	C	P	Si	Co	S	Fe
Composition, wt.%	8.14	1.43	18.02	0.045	0.029	0.44	0.41	0.0005	Balance

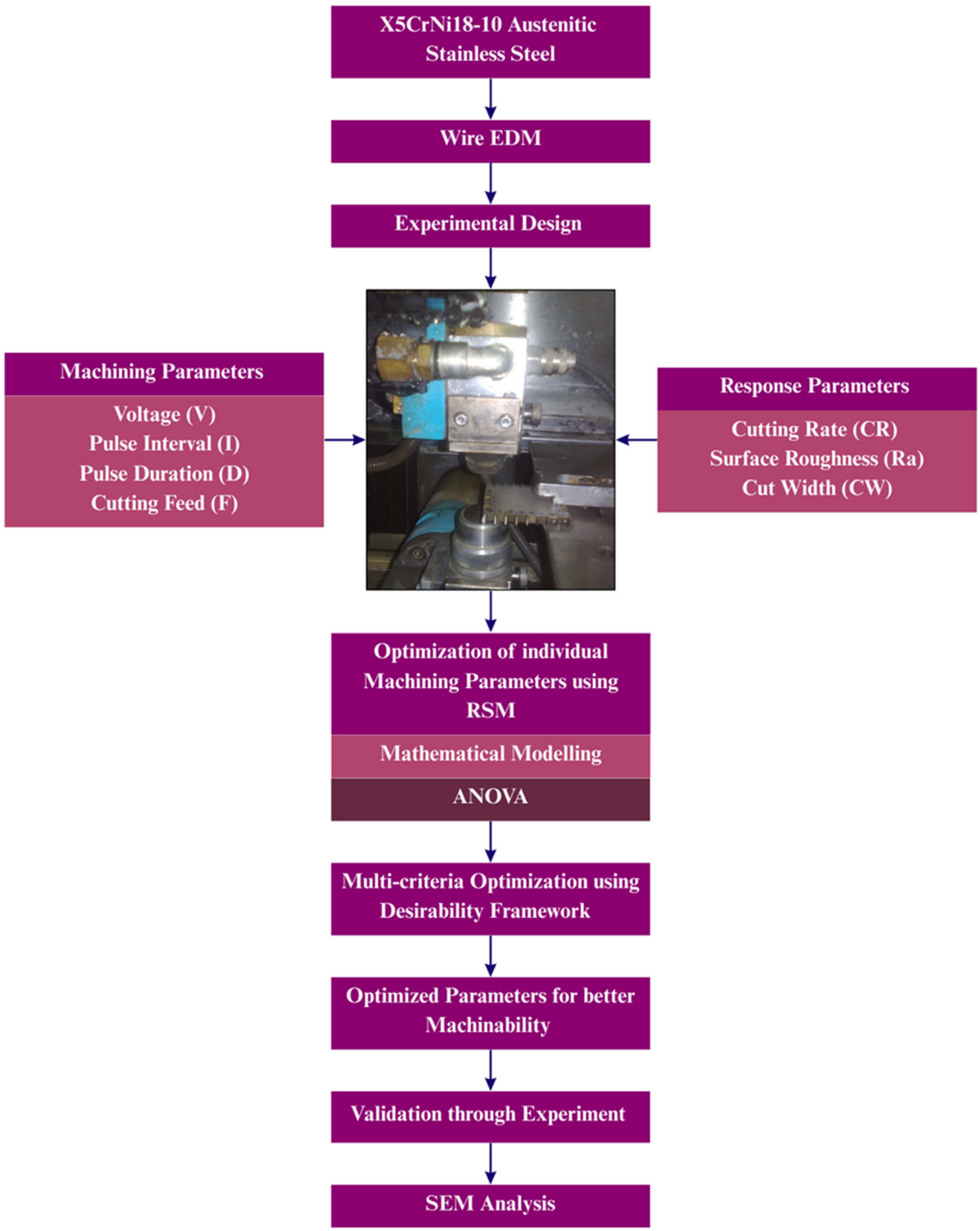

Fig. 1 Schematic flowchart of the experimental methodology and optimization procedure implemented in this study

0.8 mm was used during the measurement, in line with ISO 4288 guidelines. This specific cut-off is recommended for Ra values ranging from 0.1 to 2.0 μm, as it effectively captures the relevant surface texture while filtering out broader waviness that could distort the results (Ref 24). Choosing the right cut-off length is crucial to ensure consistent, reliable, and comparable

surface roughness data. To account for surface variability, measurements were taken at three random locations on the machined surface, and the average Ra value was used for further analysis. Cut/kerf width was determined using a Video Measuring System (Model 2010F). Table 2 provides the selected machining parameters, including their corresponding units, variation ranges, and symbols used in this study. To further assess surface morphology, Scanning Electron Microscopy (SEM) was performed using a JEOL 6700 instrument on the Wire EDM-machined surfaces.

2.3 Response Surface Methodology

Response Surface Methodology (RSM) is a powerful mathematical and statistical approach used to develop predictive models and optimize multiple performance characteristics of a process governed by several input parameters and output responses. Through RSM, regression models are constructed to establish the relationship between process variables and performance metrics (Ref 25). The methodology allows for the evaluation of both individual and combined (interactive) effects of process parameters, as well as their second-order (quadratic) influence on the responses. These effects can be visualized graphically using a quadratic response surface equation. Box–Behnken Design (BBD) was chosen for this study because of its practical advantages in RSM-based optimization. Compared to alternatives like the Central Composite Design (CCD), BBD is more efficient; it requires fewer experimental runs for the same number of factors, which helps save time and resources while still allowing for accurate modeling of quadratic relationships. Another key benefit of BBD is that it avoids extreme corner points in the design space (Ref 24). In the context of Wire EDM, this is especially important, as running experiments at extreme parameter combinations could lead to unstable or unsafe conditions, such as wire breakage. By keeping all design points within a more controlled and practical range, BBD provides a safer and more robust framework for experimentation. To ensure the results were both statistically reliable and reproducible, the study incorporated both repetition and replication. Repetition involved taking three Ra measurements at different spots on each machined specimen and averaging them. Replication was done by repeating the center point of the design five times in a randomized order, which helped estimate pure error and confirm the consistency of the process over time.

The general form of the second-order polynomial model used in RSM is expressed as follows in Eq 1 (Ref 26):

$$Y_i = S_0 + \sum_{i=1}^{n} S_i X_i + \sum_{i=1}^{n} S_{ii} X_i^2 + \sum_{i<j}^{3} S_{ij} X_i X_j \quad \text{(Eq 1)}$$

where Y_i is the predicted response, S_0 is the constant term, are the process variables, X_i are the process variables, S_i, S_{ii}, S_{ij} represent the regression coefficients for the linear, quadratic, and interaction terms, respectively. In the present study, RSM is applied to analyze the influence of key Wire EDM parameters, Voltage (V), Pulse Interval (I), Pulse Duration (D), and Cutting Feed (F), on three critical performance responses during the machining of X5CrNi18-10 ASS. Using experimental data, mathematical models for each response are developed through RSM. The statistical validity and adequacy of the derived models are subsequently evaluated using ANOVA. The decision to use a quadratic model in this study was intentional and grounded in the nature of the Wire EDM process. Manufacturing methods like this often involve complex, nonlinear interactions between input parameters and output responses due to factors such as thermal erosion, spark behavior, and debris flushing. A simple linear model would fall short in capturing these nuanced relationships, especially when there is curvature in the response surface. A quadratic model, on the other hand, includes squared and interaction terms, making it the most straightforward option capable of modeling this complexity. It also helps in identifying optimal parameter settings that might lie within the experimental space, rather than just at the extremes. Furthermore, the BBD was chosen because it efficiently supports the estimation of a quadratic model. The effectiveness of this approach was later validated through ANOVA to confirm the significance of the quadratic and interaction terms for key responses.

Table 2 Wire EDM machining parameters and their variation levels

Parameter	Unit	Minimum	Maximum
Voltage (V)	volt	55	65
Pulse interval (I)	μs	40	50
Pulse duration (D)	μs	100	120
Cutting feed (F)	m/min	1	9

2.4 Desirability Framework

Selecting the optimal combination of process parameters is a challenging task, particularly when multiple performance characteristics must be optimized simultaneously. Optimizing each response individually often leads to different sets of process conditions, where improving one performance metric may compromise others. To address this, numerical optimization using the desirability function approach is employed in this study to achieve simultaneous optimization of multiple performance characteristics, namely CR, Ra, and CW. This technique transforms each predicted response into a dimensionless desirability value, ranging between 0 and 1. A desirability value of 0 indicates that the corresponding response falls outside the acceptable range, while a value of 1 signifies a fully desirable response (Ref 27). The desirability functions are defined based on the nature of the response—either to be maximized (e.g., cutting rate) or minimized (e.g., surface roughness and cut width). The overall or composite desirability (D) is calculated as the geometric mean of the individual desirability values. It is expressed in Eq 2 (Ref 28):

$$D = (d_1 \times d_2 \times d_3 \times \dot{s} \times d_n)^{1/n} \quad \text{(Eq 2)}$$

Additionally, the method allows assigning importance levels to each response to reflect their relative priority in the optimization process. The importance rating ranges from 1 (+) for least important to 5 (+++++) for highly important responses. If no particular preference is given, a medium importance level of 3 (+++) is typically used. The optimal process parameter settings are those that yield the maximum composite desirability value.

3. Results and Discussion

Table 3 presents the experimental design based on the Box–Behnken Design (BBD) and the corresponding observed responses for the Wire EDM of X5CrNi18-10 ASS. The

Table 3 Experimental design matrix based on BBD with actual parameter settings and measured responses

		Machining Parameters				Response parameters		
		Voltage (V)	Pulse interval (I)	Pulse duration (D)	Cutting feed (F)	Cutting rate(CR)	Surface roughness (Ra)	Cut width (CW)
Std	Run	volt	μs	μs	m/min	mm^3/min	μm	mm
21	1	60	40	110	1	37.9507	1.34	0.316
18	2	65	45	100	5	32.3102	0.72	0.312
8	3	60	45	120	9	48.7805	4.39	0.327
13	4	60	40	100	5	28.4495	0.11	0.307
2	5	65	40	110	5	46.2963	2.01	0.322
27	6	60	45	110	5	45.8716	1.77	0.32
28	7	60	45	110	5	45.977	1.79	0.32
5	8	60	45	100	1	24.6305	0.13	0.305
10	9	65	45	110	1	37.8072	1.33	0.316
6	10	60	45	120	1	39.8406	1.4	0.318
4	11	65	50	110	5	31.7965	0.71	0.311
16	12	60	50	120	5	38.9105	1.35	0.317
22	13	60	50	110	1	36.1664	1.03	0.314
14	14	60	50	100	5	30.8166	0.44	0.308
15	15	60	40	120	5	48.0769	4.81	0.337
7	16	60	45	100	9	44.7427	1.58	0.319
25	17	60	45	110	5	44.9438	1.51	0.318
23	18	60	40	110	9	46.729	3.18	0.336
24	19	60	50	110	9	37.6648	1.256	0.315
3	20	55	50	110	5	36.5631	1.12	0.315
12	21	65	45	110	9	44.6429	1.48	0.318
19	22	55	45	120	5	43.8596	1.42	0.318
1	23	55	40	110	5	46.2963	1.88	0.321
11	24	55	45	110	9	46.62	2.37	0.338
26	25	60	45	110	5	46.0829	1.83	0.32
17	26	55	45	100	5	35.9712	1.01	0.313
20	27	65	45	120	5	46.729	2.48	0.324
29	28	60	45	110	5	46.5116	2.17	0.33
9	29	55	45	110	1	38.835	1.35	0.317

design matrix systematically varies the four machining parameters across their defined levels. The design includes five replicated runs at the center point (Runs 6, 7, 17, 25, and 28) to quantify experimental error. The resulting machining performance is evaluated based on three key response variables: CR in mm^3/min, Ra in μm, and CW in mm. A preliminary observation of the results reveals considerable variation in the response variables across the 27 experimental runs. For instance, the CR ranges from a minimum of 24.6305 mm^3/min (Run #8) to a maximum of 48.7805 mm^3/min (Run #3). This substantial variation suggests a significant influence of the chosen machining parameters and their interactions on the material removal process. Similarly, Ra values span from a low of 0.11 μm (Run #4) to a high of 4.81 μm (Run #15), indicating a strong dependence on the machining conditions. The CW also exhibits variability, ranging from 0.305 mm (Run #8) to 0.338 mm (Run #24), highlighting the impact of the parameters on the dimensional accuracy of the machined slot. The experimental data presented in Table 3 serve as the foundation for developing predictive models using RSM. By analyzing the relationship between the input parameters and the output responses, it is possible to quantify the individual and interactive effects of voltage, pulse interval, pulse duration, and cutting feed on the CR, Ra, and CW.

3.1 RSM Optimization of Cutting Rate (CR)

Figure 2 presents diagnostic plots evaluating the adequacy of the developed model for predicting CR in the Wire EDM of X5CrNi18-10 ASS. Figure 2(a) shows the residuals versus the run number. A random scatter of residuals around zero with no discernible pattern (such as curvature) indicates that the model effectively captures the underlying relationship between the machining parameters and CR and that the errors are independent and identically distributed. The red boundary lines at ± 3.93041 indicate the threshold for externally studentized residuals. Nearly all residuals fall within these bounds, suggesting the absence of significant outliers and further affirming model adequacy. Figure 2(b) depicts predicted CR values against actual observed CR values. Ideally, data points should cluster around the 45º diagonal line representing perfect agreement. The close alignment of the points with this line confirms a strong correlation and good predictive accuracy (Ref 29).

Table 4 presents the ANOVA for the quadratic model developed to predict CR in the Wire EDM of X5CrNi18-10 ASS. The quadratic model demonstrates strong statistical significance, as evidenced by a high model F value of 10.70 and a p value of < 0.0001. This indicates that the model captures a substantial portion of the variability in the CR, with a very low probability that this result is due to random chance.

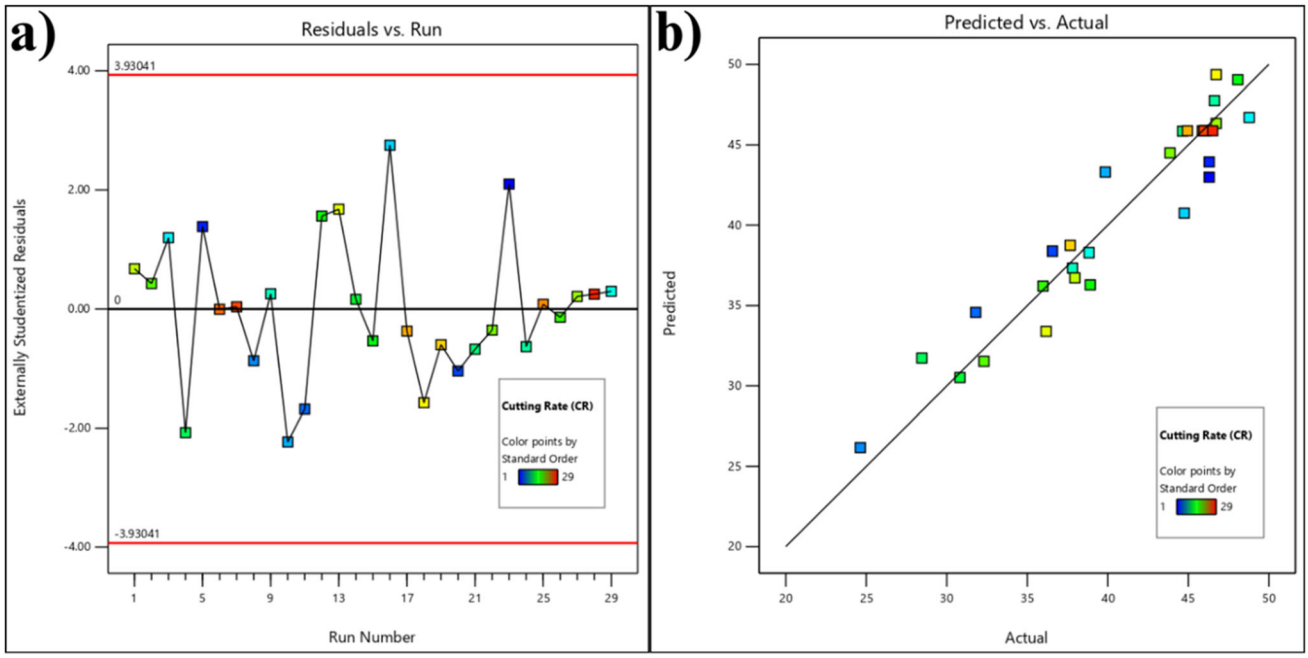

Fig. 2 Diagnostic plots for the CR quadratic model: (a) Residuals vs. Run, and (b) Predicted vs. Actual CR values

Table 4 ANOVA results for the quadratic model of CR

Source	Sum of Squares	*df*	Mean Square	*F* value	*p* value	
Model	1111.61	14	79.40	10.70	< 0.0001	Significant
A: Voltage (V)	6.11	1	6.11	0.8231	0.3796	
B: Pulse Interval (I)	146.17	1	146.17	19.69	0.0006	
C: Pulse Duration (D)	399.93	1	399.93	53.87	< 0.0001	
D: Cutting Feed (F)	242.55	1	242.55	32.67	< 0.0001	
AB	5.68	1	5.68	0.7651	0.3965	
AC	10.66	1	10.66	1.44	0.2507	
AD	0.2253	1	0.2253	0.0303	0.8642	
BC	33.26	1	33.26	4.48	0.0527	
BD	13.25	1	13.25	1.78	0.2029	
CD	31.21	1	31.21	4.20	0.0596	
A^2	16.12	1	16.12	2.17	0.1627	
B^2	121.49	1	121.49	16.36	0.0012	
C^2	140.41	1	140.41	18.91	0.0007	
D^2	25.71	1	25.71	3.46	0.0839	
Residual	103.93	14	7.42			
Lack of Fit	102.61	10	10.26	30.95	0.0024	Significant
Pure Error	1.33	4	0.3315			
Cor Total	1215.55	28				
Std. Dev.	2.72		R^2		0.9145	
Mean	40.69		Adjusted R^2		0.8290	
C.V. %	6.70		Predicted R^2		0.5121	
			Adeq Precision		11.8356	

The *R*-squared (R^2) value of 0.9145 further supports the model's adequacy, showing that 91.45% of the total variation in CR is explained by the model. The adjusted R^2 value of 0.8290, which accounts for the number of predictors, remains relatively high, suggesting that the model is not overfitted and that the key influential terms have been correctly included. However, there is a noticeable drop to a predicted R^2 value of 0.5121. Despite this, the adequate precision value of 11.8356, which measures the signal-to-noise ratio, is well above the recommended threshold of 4. This indicates that the model has a sufficient signal for navigating the design space. The Coefficient of Variation (C.V.) of 6.70% also reflects good precision and reliability in the experimental results.

The ANOVA results reveal that pulse duration and cutting feed have the most statistically significant linear effects on CR, both with *p* values of < 0.0001 (Ref 30). Pulse interval also shows a significant linear effect ($p = 0.0006$). Additionally, the quadratic terms for pulse interval (*I*) (B^2, $p = 0.0012$) and pulse

duration (D) (C^2, $p = 0.0007$) are highly significant, indicating nonlinear relationships between these factors and the CR. The quadratic effect of cutting feed (F) (D^2) is marginally significant ($p = 0.0839$), suggesting a potential but less pronounced nonlinear influence. Among the interaction terms, only the interaction between pulse interval (I) and cutting feed (F) (BD) is statistically significant ($p = 0.0209$), implying that the influence of one parameter is dependent on the level of the other. Other interaction terms, such as those involving Voltage (AB, AC, AD), as well as interactions like BC and CD, are not statistically significant, with p values exceeding the 0.05 threshold. Furthermore, the linear and quadratic effects of voltage (A and A^2) are not significant, indicating that within the tested range, voltage has minimal influence on the cutting rate.

$$\begin{aligned} CR = {} & -1387.9693149481 + (6.0363949166692 \times V) \\ & + (24.540079416669 \times I) + (11.797961541667 \times D) \\ & + (14.8561890625 \times F) - (0.04766600000002 \times V \times I) \\ & + (0.032651999999997 \times V \times D) \\ & - (0.01186625 \times V \times F) \\ & - (0.057667500000004 \times I \times D) \\ & - (0.090998750000001 \times I \times F) \\ & - (0.069826875 \times D \times F) \\ & - \left(0.063054433333344 \times V^2\right) \\ & - \left(0.17310793333335 \times I^2\right) \\ & - \left(0.046525483333333 \times D^2\right) \\ & - \left(0.12443661458333 \times F^2\right) \end{aligned} \quad \text{(Eq 3)}$$

Equation 3 represents the quadratic regression model developed using RSM to predict the CR. The linear coefficients (positive in all four cases) suggest that increases in parameters generally led to increases in the CR. Notably, the coefficients for pulse interval (24.54) and cutting feed (14.86) are comparatively large, indicating a strong positive influence on CR. Pulse duration (11.80) also exerts a considerable positive effect, while voltage (6.04), though positive, was shown to be statistically insignificant in the ANOVA, implying its contribution may be less reliable across the experimental domain. The interaction terms (e.g., $V \times I$, $V \times D$, $V \times F$, $I \times D$, $I \times F$, $D \times F$) have smaller coefficients compared to the linear terms, indicating that the combined effects of two parameters on CR are less pronounced than their individual contributions. Most interaction coefficients are negative, which suggests a synergistic dampening effect—meaning that the simultaneous increase of two parameters does not lead to a proportionate increase in CR. For example, the interaction term $V \times I$ with a coefficient of − 0.0477 implies that increasing both voltage and pulse interval together may not yield the same gain in CR as when increased independently. The quadratic terms (V^2, I^2, D^2, F^2) all have negative coefficients, revealing that the relationships between the machining parameters and CR are not strictly linear but exhibit curvature. These negative coefficients indicate the presence of diminishing returns; that is, increasing a parameter beyond a certain point may reduce the CR rather than enhance it. Among them, the quadratic term for Pulse Interval (I^2) shows the most significant curvature effect with a relatively large negative coefficient (− 0.1731), suggesting that the pulse interval must be carefully optimized to avoid efficiency losses. Overall, the regression model offers a comprehensive quantitative relationship between the Wire EDM process parameters and the CR.

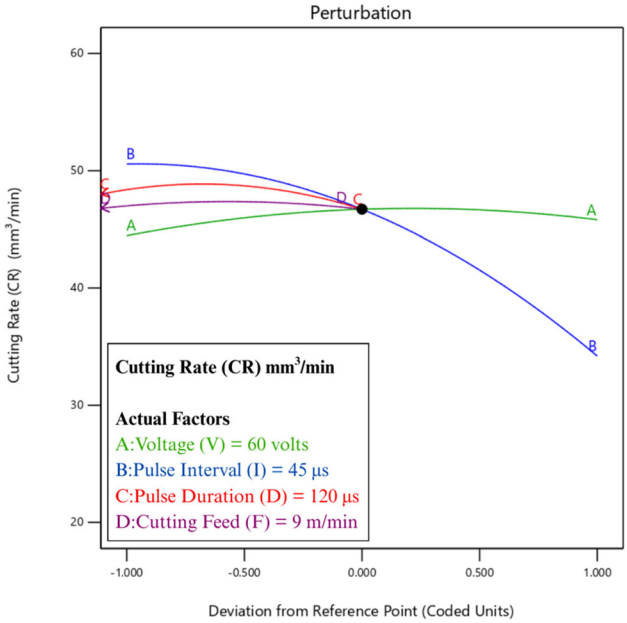

Fig. 3 Perturbation plot illustrating the sensitivity of CR

Figure 3 illustrates the perturbation plot that visualizes the sensitivity of CR to changes in each individual machining parameter by varying one parameter at a time across its coded range (from − 1 to + 1), while keeping the others fixed at their reference values. These reference values correspond to actual settings of 60 volts for voltage, 45 μs for pulse interval, 120 μs for pulse duration, and 9 m/min for cutting feed. The observed CR spans from a minimum of 24.6305 mm^3/min (Run #8) to a maximum of 48.7805 mm^3/min (Run #3) (Table 3), providing context for interpreting changes depicted in the plot. The slope of each curve in the perturbation plot indicates how strongly the CR responds to changes in the associated parameter. Among all the factors, Curve B, representing pulse interval, shows the steepest downward slope on both sides of the reference point. This indicates that CR is highly sensitive to variations in pulse interval around 45 μs. Either increasing or decreasing the pulse interval from this point causes a notable decline in CR, suggesting that maximum CR occurs near the lower end of the tested pulse interval range. This finding is consistent with the regression analysis, which highlighted the significant linear and quadratic influence of this parameter. Curve C, corresponding to pulse duration, exhibits a moderately steep slope. Deviations from the reference point of 120 μs—particularly reductions—result in a decline in CR, indicating that higher pulse duration settings tend to yield better performance. The maximum CR in this case appears to be achieved at or near the upper limit of the pulse duration range, reinforcing its positive contribution to material removal rate (Ref 31). In contrast, Curve D, representing cutting feed, shows a relatively flat trend around the reference value of 9 m/min, with only a slight downward curvature at the extremes. This implies that CR is less sensitive to variations in cutting feed near this point, although the trend still favors higher values within the tested range. Curve A, which represents voltage, displays the flattest response across its range. This suggests that voltage has the least impact on CR around the reference value of 60 volts, with only minor variations observed in response to changes. This observation aligns with the ANOVA results, which showed

voltage to be statistically insignificant within the studied parameter space.

Figure 4 presents a set of three-dimensional response surface plots that illustrate the interactive effects of various pairs of machining parameters on the CR during the Wire EDM of X5CrNi18-10 ASS. The surface color gradient from cool (blue) to warm (red) indicates the magnitude of the CR, with warmer colors corresponding to higher CR values. The projected contour plots on the base plane offer a two-dimensional perspective, and the red dot marks the predicted maximum CR in each parameter combination. In Fig. 4(a), pulse duration and cutting feed are held constant at 110 μs and 5 m/min, respectively. The surface indicates that pulse interval has a dominant effect on the CR, with lower values yielding higher CR across nearly the entire voltage range. Although voltage shows a slight positive influence, particularly at lower pulse intervals, its overall effect is relatively minor. A strong interaction is observed between the voltage and pulse interval, meaning the effect of voltage on CR is more pronounced when the pulse interval is reduced. The maximum CR is predicted by the combination of a low pulse interval and high voltage. In Figure 4(b), the pulse interval is fixed at 45 μs and the cutting feed at 5 m/min. The surface reveals that pulse duration plays a significant role, with CR increasing steadily as pulse duration rises. Voltage continues to have a secondary effect, showing a slight upward trend in CR at higher values. This interaction is less pronounced than in Fig. 4(a), but the surface still indicates that the benefit of increasing pulse duration is marginally enhanced by higher voltage. The maximum CR occurs at the upper bounds of both voltage and pulse duration.

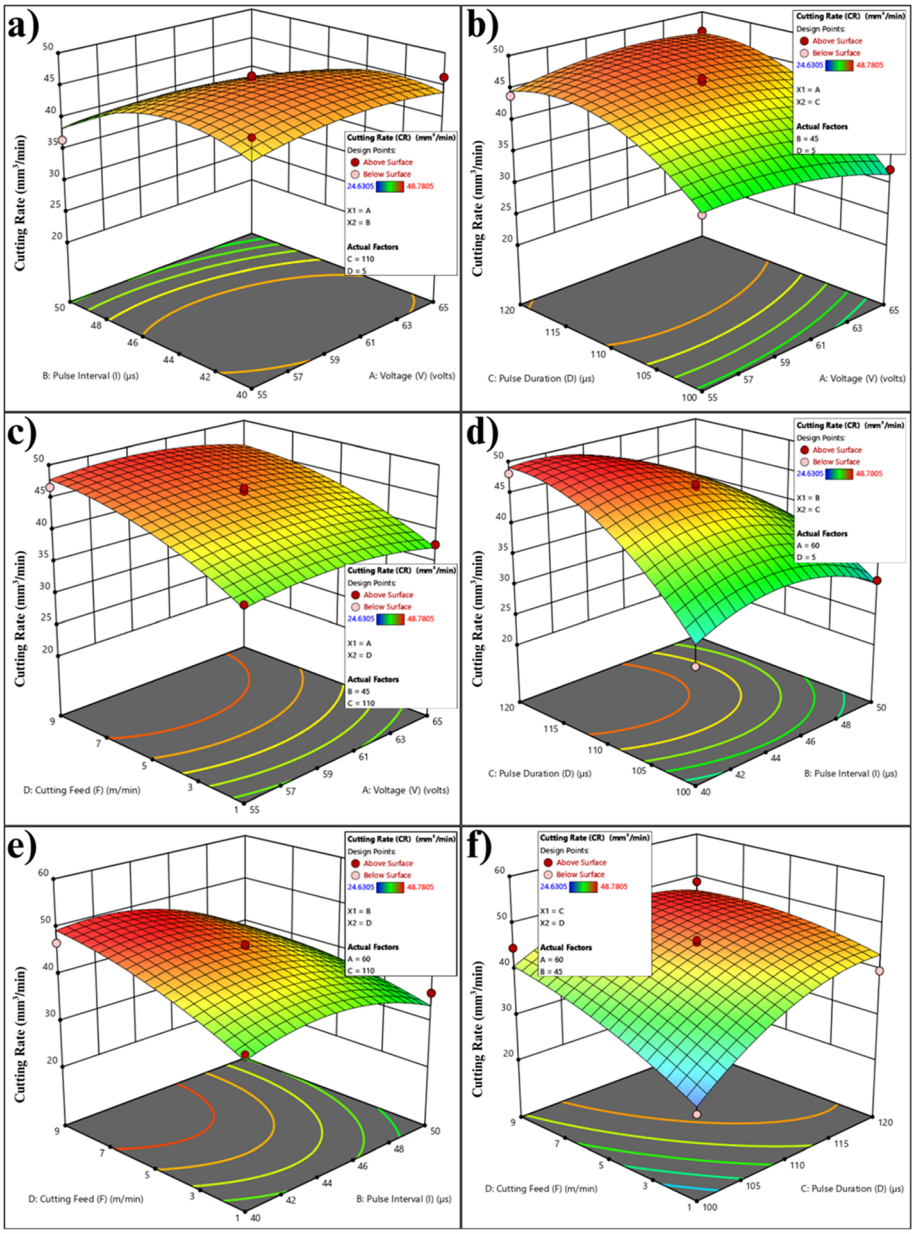

Fig. 4 3D response surface plots showing the interactive effects of parameter pairs on CR: (a) Voltage and Pulse Interval, (b) Voltage and Pulse Duration, (c) Voltage and Cutting Feed, (d) Pulse Interval and Pulse Duration, (e) Pulse Interval and Cutting Feed, and (f) Pulse Duration and Cutting Feed (color figure online)

With pulse interval and pulse duration set to 45 and 110 μs, respectively, this plot shows that cutting feed has a strong positive effect on the CR (Fig. 4c). CR consistently increases with higher cutting feed values across all levels of voltage. Voltage, again, plays a relatively minor role but shows a modest positive influence, especially at higher cutting feeds. The surface indicates a mostly additive interaction, where the maximum CR is achieved at high cutting feed and high voltage. This plot (Fig. 4d), with voltage set at 59 volts and cutting feed at 5 m/min, emphasizes the significant influence of both pulse interval and pulse duration. CR increases with higher pulse duration and decreases with higher pulse interval, confirming their opposing effects. A clear interaction is evident: the benefit of increasing pulse duration is much greater at lower pulse intervals. The predicted maximum CR lies at the combination of low pulse interval and high pulse duration, highlighting the synergistic effect of these two parameters.

With voltage at 59 volts and pulse duration at 110 μs, this plot demonstrates a strong positive influence of cutting feed and a negative influence of pulse interval on the CR (Fig. 4e). The interaction is substantial; cutting feed's positive impact is much more pronounced when the pulse interval is low. This reinforces the earlier observations that minimizing pulse interval and maximizing cutting feed yield optimal results. The maximum CR is observed at high cutting feed and low pulse interval. In this final plot (Fig. 4f), voltage is held at 59 volts and pulse interval at 45 μs. Both pulse duration and cutting feed positively affect the CR, and the surface shows a relatively smooth and uniform increase in CR with rising values of both parameters. Unlike the more complex interactions involving pulse interval, the relationship here is more straightforward, with both parameters contributing independently to higher CR. The maximum CR is attained at high values for pulse duration and cutting feed. Together, these response surface plots reveal important trends in the behavior of the Wire EDM process. The most influential parameters for increasing the CR are pulse interval (inverse relationship), pulse duration, and cutting feed (both direct relationships). Voltage, while included in all plots, consistently shows a weaker effect across the experimental range.

3.2 RSM Optimization of Surface Roughness (Ra)

Figure 5(a) displays the residuals, defined as the differences between experimentally observed Ra values and those predicted by the RSM model, plotted against the experimental run number. The residuals in this plot appear to be evenly distributed around the zero line, indicating no visible pattern or bias. This suggests that the model errors are independent and identically distributed, fulfilling a key assumption of regression modeling. Additionally, the red lines representing the bounds for externally studentized residuals ($\pm$ 3.93041) encompass the vast majority of residuals. This implies the absence of significant outliers, meaning no data points exert undue influence on the model fit. Figure 5(b) compares the predicted Ra values from the RSM model with the experimentally observed values. In this plot, the points fall reasonably close to the diagonal, indicating a strong correlation between the predicted and actual surface roughness values.

Table 5 presents the ANOVA results for the quadratic model developed to predict the Ra. The model demonstrates statistical significance with an F value of 7.41 and a corresponding p value of 0.0003. This low p value indicates that the model explains a significant portion of the observed variation in surface roughness and that the likelihood of this result occurring by random chance is very small. This supports the overall validity of the model within the experimental conditions. The goodness-of-fit statistics further reinforce this conclusion. The R^2 value of 0.8811 indicates that 88.11% of the variability in surface roughness is accounted for by the

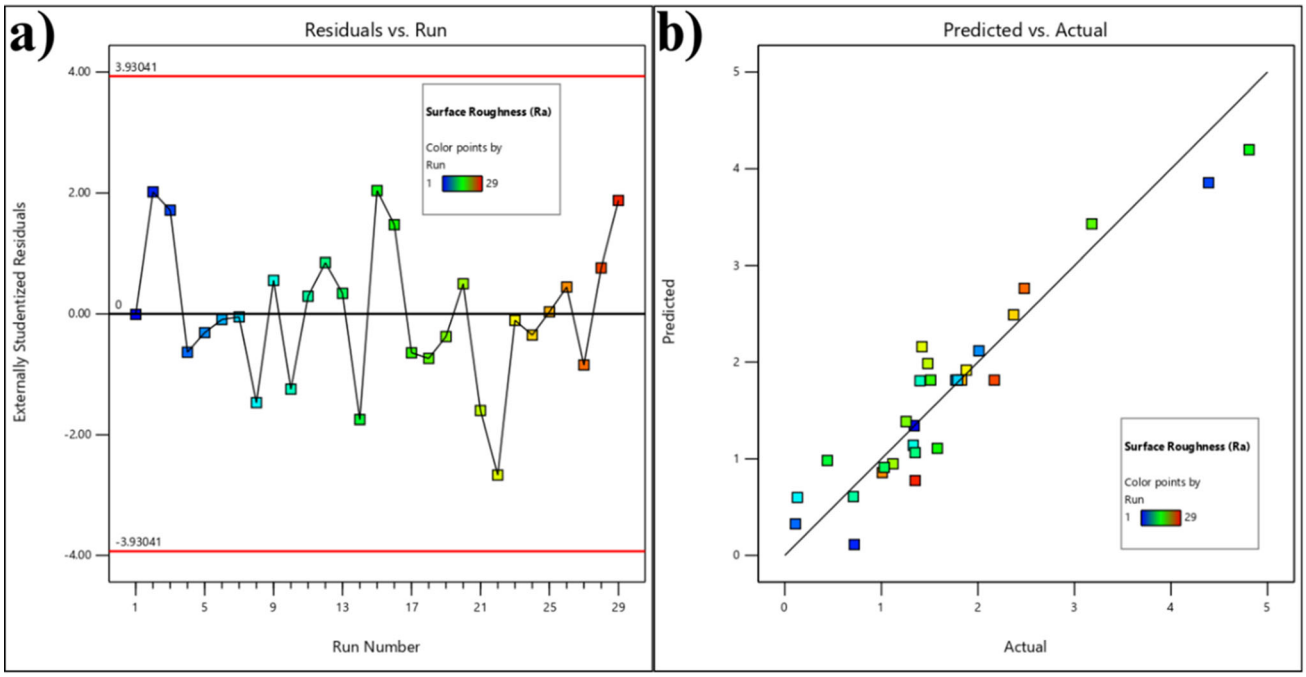

Fig. 5 Diagnostic plots for the Ra quadratic model: (a) Residuals vs. Run, and (b) Predicted vs. Actual Ra values

Table 5 ANOVA results for the quadratic model of Ra

Source	Sum of Squares	*df*	Mean Square	*F*-value	*p*-value	
Model	27.52	14	1.97	7.41	0.0003	Significant
A: Voltage (V)	0.0147	1	0.0147	0.0554	0.8173	
B: Pulse Interval (I)	4.59	1	4.59	17.32	0.0010	
C: Pulse Duration (D)	11.72	1	11.72	44.21	< 0.0001	
D: Cutting Feed (F)	4.91	1	4.91	18.52	0.0007	
AB	0.0729	1	0.0729	0.2749	0.6083	
AC	0.4556	1	0.4556	1.72	0.2110	
AD	0.1892	1	0.1892	0.7136	0.4125	
BC	3.59	1	3.59	13.54	0.0025	
BD	0.6512	1	0.6512	2.46	0.1394	
CD	0.5929	1	0.5929	2.24	0.1570	
A^2	0.5556	1	0.5556	2.10	0.1698	
B^2	0.0984	1	0.0984	0.3711	0.5522	
C^2	0.0147	1	0.0147	0.0556	0.8170	
D^2	0.0383	1	0.0383	0.1444	0.7096	
Residual	3.71	14	0.2652			
Lack of Fit	3.49	10	0.3490	6.29	0.0456	Significant
Pure Error	0.2219	4	0.0555			
Cor Total	31.23	28				
Std. Dev.	0.5149		R^2		0.8811	
Mean	1.65		Adjusted R^2		0.7623	
C.V. %	31.13		Predicted R^2		0.3452	
			Adeq Precision		11.0298	

model. The adjusted R^2 value of 0.7623, which adjusts for the number of predictors in the model, remains relatively high and suggests that the most meaningful terms have been included. However, the predicted R^2 value is notably lower at 0.3452. The adequate precision value of 11.0298, which measures the signal-to-noise ratio, exceeds the recommended threshold of 4, confirming that the model has a sufficiently strong signal and can be used to explore the design space. However, the C.V. of 31.13% is relatively high, indicating a greater degree of dispersion in the surface roughness data compared to other responses, such as CR. One concern highlighted by the ANOVA is the significant lack of fit, with an F value of 6.29 and a p value of 0.0456. A significant lack of fit implies that the model does not fully capture all the complexities of the data and suggests that other effects, such as higher-order terms or additional variables, may be necessary for improved modeling accuracy.

Examining the significance of individual model terms reveals that pulse duration ($p < 0.0001$) and cutting feed ($p = 0.0007$) have the most substantial linear effects on Ra (Ref 32). Pulse interval is also a significant factor ($p = 0.0010$), though to a lesser extent. Additionally, the interaction between pulse interval (I) and pulse duration (D) (BC) is statistically significant ($p = 0.0025$), suggesting that the effect of one variable depends on the level of the other. In contrast, several terms were found to be statistically insignificant. Voltage ($p = 0.8173$) does not significantly affect Ra, nor do its interactions with other parameters or its quadratic term. Similar non-significant results were observed for other interaction and quadratic terms, such as AB, AC, AD, BD, CD, A^2, B^2, C^2, and D^2. These findings suggest that linear and specific interaction effects dominate the model, while higher-order and voltage-related terms have limited influence within the studied range.

$$\begin{aligned}\mathrm{Ra} = &-127.97799 + (0.952675 \times V) + (2.82904 \times I) \\ &+ (0.603325 \times D) + (0.613521 \times F) - (0.005400 \times V \times I) \\ &+ (0.006750 \times V \times D) - (0.010875 \times V \times F) \\ &- (0.018950 \times I \times D) - (0.020175 \times I \times F) \\ &+ (0.009625 \times D \times F) - \left(0.011707 \times V^2\right) \\ &- \left(0.004927 \times I^2\right) - \left(0.000477 \times D^2\right) + \left(0.004802 \times F^2\right)\end{aligned} \quad \text{(Eq 4)}$$

Equation 4 represents the developed quadratic regression model for predicting Ra in the Wire EDM of X5CrNi18-10 ASS. The linear terms in the model carry the greatest influence, particularly for pulse interval, pulse duration, and cutting feed. The coefficient for voltage (0.952675) is positive, indicating that surface roughness tends to increase slightly with voltage. However, ANOVA results showed that voltage is not a statistically significant factor, and thus its influence is likely limited or inconsistent within the tested range. In contrast, pulse interval has a large positive coefficient (2.82904), indicating a strong and significant effect—higher pulse intervals lead to rougher surfaces. Pulse duration and cutting feed also exhibit positive coefficients (0.603325 and 0.613521, respectively), suggesting that increasing either of these parameters contributes to increased Ra. Both were identified as highly significant linear terms in the ANOVA. The interaction terms capture how pairs of parameters jointly influence surface roughness. These coefficients are generally smaller than the linear terms, indicating less pronounced but still relevant combined effects. Negative interaction coefficients, such as for voltage × pulse interval (− 0.005400), voltage × cutting feed (− 0.010875), and pulse interval × pulse duration (− 0.018950), suggest a mitigating or synergistic interaction. This means that the combined influence of increasing both parameters is less than the sum of their individual effects, potentially leading to a more

stable or reduced roughness. Conversely, positive coefficients like those for voltage × pulse duration (0.006750), pulse interval × cutting feed (0.020175), and pulse duration × cutting feed (0.009625) imply antagonistic interactions, where the combination of increased values leads to greater surface roughness. Among these, only the interaction between pulse interval and pulse duration (BC) was found to be statistically significant in the ANOVA. The quadratic terms in the model reveal nonlinear relationships between each parameter and surface roughness. The negative coefficients for voltage^2 (− 0.011707) and pulse interval^2 (− 0.004927) indicate a downward curvature, implying that there may be a peak beyond which further increases in these parameters begin to reduce Ra slightly. Meanwhile, the positive coefficients for pulse duration^2 (0.000477) and cutting feed^2 (0.004802) suggest a slight upward curvature, indicating an accelerating increase in roughness at higher levels of these parameters. Despite these mathematical trends, none of the quadratic terms were statistically significant based on the ANOVA, meaning their influence on Ra is likely minor within the studied range.

The perturbation plot of Ra is centered around a defined reference point where Voltage (A) = 60 volts, Pulse Interval (B) = 40 μs, Pulse Duration (C) = 100 μs, and Cutting Feed (D) = 5 m/min (Fig. 6). Among the four parameters, Pulse Duration (C), represented by the red curve, demonstrates the most significant influence on Ra. As pulse duration increases from the reference value, Ra rises sharply, indicating a strong positive relationship. Conversely, reducing pulse duration results in a marked decrease in surface roughness. This steep response highlights that controlling pulse duration near its lower bound is crucial for achieving a smoother machined surface, making it the most critical factor among those studied. The Pulse Interval (B), depicted by the blue curve, also shows a clear upward trend in Ra as it deviates positively from the reference point. Lower pulse intervals contribute to smoother surfaces, reinforcing its importance as a significant factor influencing Ra. While not as steep as pulse duration, the slope of the curve still suggests a considerable impact on surface

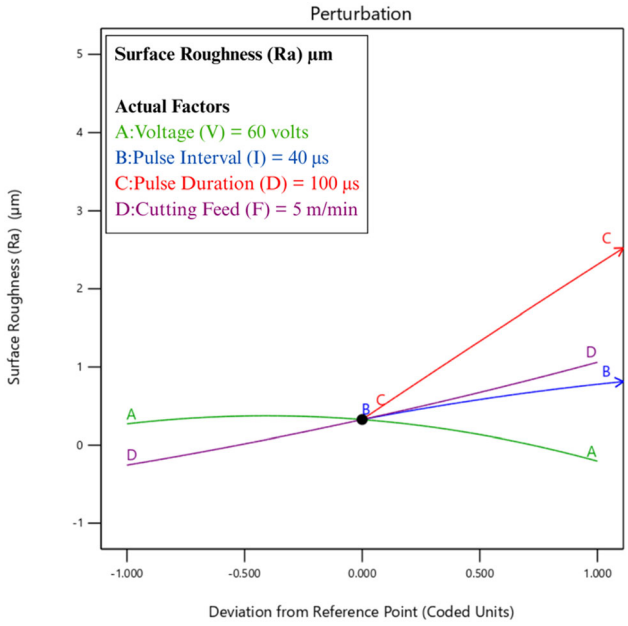

Fig. 6 Perturbation plot illustrating the sensitivity of Ra

finish, particularly within the tested range of 40-50 μs. The Cutting Feed (D), shown as the purple curve, follows a similar pattern. Increasing the cutting feed results in a moderate increase in Ra, while reducing it leads to improved surface quality. Although the effect is less pronounced than that of pulse duration or pulse interval, it remains a relevant parameter to consider, especially when optimizing for minimal Ra. In contrast, the Voltage (A) curve, illustrated in green, is relatively flat across the range, indicating that variations in voltage around the reference value of 60 volts have little to no significant effect on Ra. This observation aligns well with the ANOVA results, which identified voltage as statistically insignificant for Ra in this experimental design. The visual representation confirms that pulse duration exerts the greatest influence on Ra, followed by pulse interval and cutting feed, while voltage has minimal impact in the vicinity of the reference point. The data also show that the parameter setting corresponding to Run #4 yields a particularly favorable Ra value of 0.11 μm, one of the lowest in the study.

Figure 7 presents a series of three-dimensional response surface plots, and the color gradient on each surface corresponds to the magnitude of Ra, with warmer colors (e.g., red) indicating higher roughness values and cooler colors (e.g., blue) indicating smoother surfaces. With pulse duration set to 110 μs and cutting feed to 5 m/min, this plot illustrates that Ra is sensitive to variations in pulse interval, with lower values leading to significantly smoother surfaces (Fig. 7a). Although voltage does influence Ra, its effect is relatively mild and more evident when pulse interval is low. The surface indicates an interaction between voltage and pulse interval, suggesting that the influence of one factor is dependent on the level of the other. The lowest Ra is predicted at the lower end of both the voltage and pulse interval, reinforcing the importance of minimizing these settings to improve surface quality. In Fig. 7b, with a pulse interval of 45 μs and a cutting feed of 5 m/min, pulse duration emerges as the dominant factor affecting Ra. The surface clearly shows that lower pulse duration results in a smoother finish. Voltage again demonstrates a modest positive influence on Ra, particularly when pulse duration is reduced. There is an interaction effect, where higher voltage levels slightly intensify the adverse impact of increased pulse duration. The minimum Ra is observed at the lower values of both voltage and pulse duration. In Fig. 7c, where pulse interval is 45 μs and pulse duration is 110 μs, it shows that cutting feed has a clear positive correlation with Ra. Increasing cutting feed leads to rougher surfaces, while lower values enhance surface finish. Voltage remains a less influential factor in this pair, with only a minor increase in Ra observed at higher voltages (Ref 33). The interaction between the two parameters appears minimal, and the predicted minimum Ra is found at the lower end of both voltage and cutting feed.

With voltage at 59 volts and cutting feed at 5 m/min, this plot highlights the substantial effect both pulse interval and pulse duration have on Ra (Fig. 7d). As either parameter increases, Ra also increases, indicating that smoother surfaces are obtained at their lower levels. The surface clearly shows an interaction, where the detrimental effect of high pulse duration is more pronounced at higher pulse intervals. The minimum Ra is predicted when both pulse interval and pulse duration are minimized, confirming their combined importance in surface finish optimization. For this plot (Fig. 7e), with voltage set to 59 volts and pulse duration at 110 μs, both pulse interval and cutting feed exert a strong positive influence on Ra. Lower

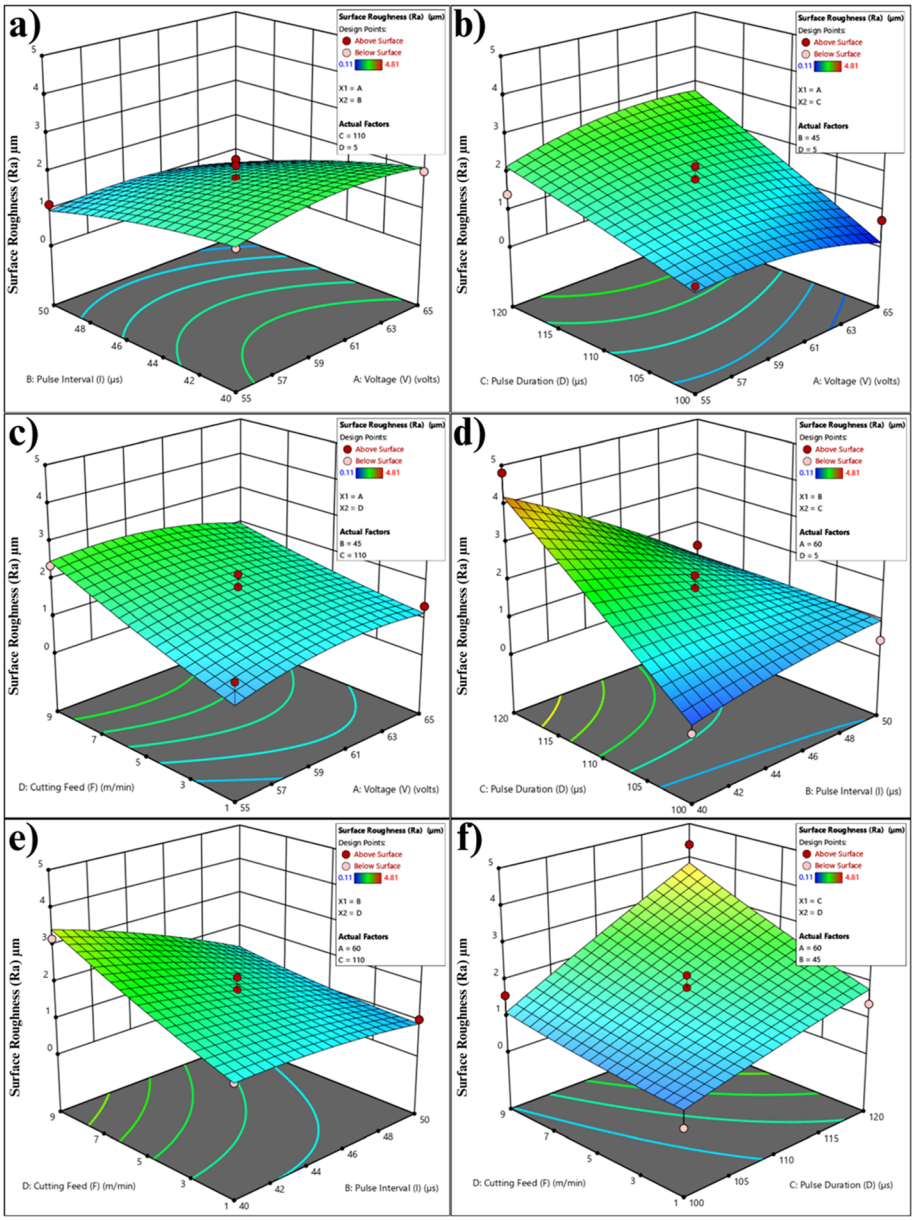

Fig. 7 3D response surface plots showing the interactive effects of parameter pairs on Ra: (a) Voltage and Pulse Interval, (b) Voltage and Pulse Duration, (c) Voltage and Cutting Feed, (d) Pulse Interval and Pulse Duration, (e) Pulse Interval and Cutting Feed, and (f) Pulse Duration and Cutting Feed

values of each parameter yield smoother surfaces, and the surface reveals a marked interaction: the roughness-increasing effect of higher pulse interval is more significant when cutting feed is also high. The predicted minimum Ra lies at the lowest tested levels of both parameters, suggesting that reducing them simultaneously is a viable approach to improving surface quality. With voltage at 59 volts and pulse interval at 45 μs, this plot confirms the positive impact of both pulse duration and cutting feed on Ra (Fig. 7f). The surface shows a relatively straightforward trend: as either parameter increases, surface roughness also increases. These visualizations serve as practical tools for selecting optimal machining conditions and emphasize that the best surface finish is achieved by minimizing pulse duration, pulse interval, and cutting feed in combination.

3.3 RSM Optimization of Cut Width (CW)

The Residuals versus Run plot illustrates the distribution of residuals, defined as the differences between the experimentally observed CW values and those predicted by the RSM model, plotted against the sequence of experimental runs (Fig. 8a). In this plot, the residuals are distributed fairly randomly and fall well within the externally studentized residual bounds ($\pm$ 3.93041). This pattern indicates that the errors are likely independent and homoscedastic (i.e., have constant variance), supporting the assumption of model adequacy. The Predicted vs. Actual plot shows the relationship between the CW values predicted by the RSM model and the experimentally observed values (Fig. 8b). Ideally, data points in this plot should lie close to the diagonal line, which represents perfect agreement

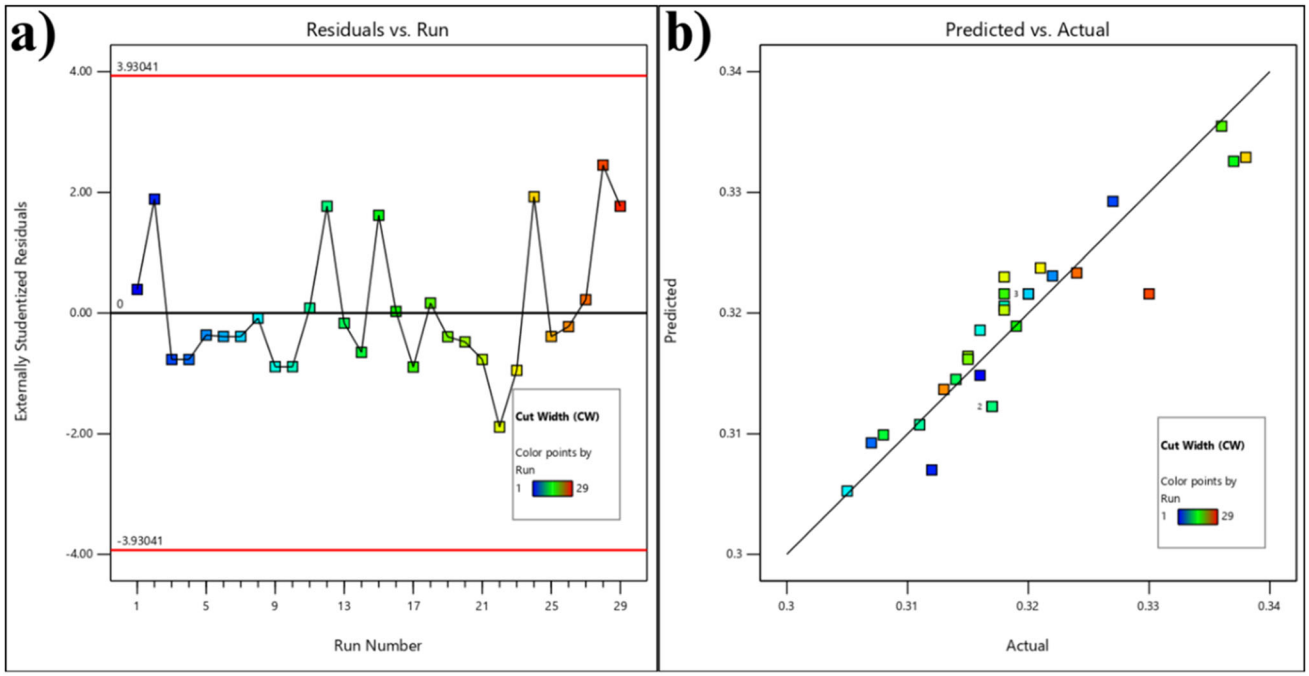

Fig. 8 Diagnostic plots for the CW quadratic model: (a) Residuals vs. Run, and (b) Predicted vs. Actual CW values

Table 6 ANOVA results for the quadratic model of CW

Source	Sum of Squares	*df*	Mean Square	*F* value	*p* value	
Model	0.0016	14	0.0001	5.80	0.0011	Significant
A: Voltage (V)	0.0000	1	0.0000	1.51	0.2394	
B: Pulse Interval (I)	0.0003	1	0.0003	14.56	0.0019	
C: Pulse Duration (D)	0.0005	1	0.0005	24.80	0.0002	
D: Cutting Feed (F)	0.0004	1	0.0004	18.78	0.0007	
AB	6.250E−06	1	6.250E−06	0.3138	0.5842	
AC	0.0000	1	0.0000	0.6150	0.4460	
AD	0.0001	1	0.0001	4.53	0.0515	
BC	0.0001	1	0.0001	5.53	0.0338	
BD	0.0001	1	0.0001	4.53	0.0515	
CD	6.250E−06	1	6.250E−06	0.3138	0.5842	
A^2	8.955E−06	1	8.955E−06	0.4496	0.5134	
B^2	0.0000	1	0.0000	1.21	0.2905	
C^2	0.0001	1	0.0001	4.40	0.0546	
D^2	2.145E−06	1	2.145E−06	0.1077	0.7477	
Residual	0.0003	14	0.0000			
Lack of Fit	0.0002	10	0.0000	0.8231	0.6363	Not significant
Pure Error	0.0001	4	0.0000			
Cor Total	0.0019	28				
Std. Dev.	0.0045		R^2		0.8530	
Mean	0.3190		Adjusted R^2		0.7060	
C.V. %	1.40		Predicted R^2		0.3550	
			Adeq Precision		9.4242	

between prediction and observation. In this case, the points are clustered closely around the diagonal, indicating a strong correlation and high predictive accuracy of the model. The residuals exhibit no systematic behavior, and the predicted values align closely with the actual measurements. This indicates that the model successfully captures the underlying relationships between the machining parameters and the resulting cut dimension.

Table 6 presents the ANOVA results for the quadratic regression model developed to predict CW, and the model demonstrates statistical significance with an F-value of 5.80 and a corresponding p-value of 0.0011. This indicates that the model explains a significant portion of the variability in CW and that the likelihood of this result arising by chance is very low. The *R*-squared (R^2) value of 0.8530 suggests that 85.30% of the variation in CW is explained by the model, indicating a good fit to the experimental data. The adjusted R^2 of 0.7060,

which accounts for the number of predictors, remains reasonably high, reinforcing the model's adequacy. However, the predicted R^2 of 0.3550 is substantially lower, pointing to limited predictive power for unseen data and a potential risk of overfitting. The adequate precision value of 9.4242, which reflects the signal-to-noise ratio, is well above the acceptable threshold of 4, confirming that the model has a strong enough signal for navigating the design space. The C.V. of 1.40% is very low, indicating excellent precision and consistency in the CW measurements.

Importantly, the lack of fit test yields an F-value of 0.8231 with a p-value of 0.6363. Since this is not statistically significant ($p > 0.05$), it suggests that the model fits well and adequately represents the observed data. This supports the model's structural validity for capturing the underlying relationship between the machining inputs and CW. The ANOVA results reveal that Pulse Duration (C) and Cutting Feed (D) are the most statistically significant parameters influencing CW, with p values of 0.0002 and 0.0007, respectively. These highly significant effects confirm that increases in either parameter result in measurable and consistent changes in CW. Pulse Interval (B) is also identified as a significant linear factor, with a p value of 0.0019, indicating a substantial contribution to variations in CW. Among interaction terms, only the BC interaction (pulse interval × pulse duration) is statistically significant ($p = 0.0338$). This implies a notable interplay between these two parameters, where the influence of one is affected by the level of the other. Interestingly, two other interactions—AD (voltage × cutting feed) and BD (pulse interval × cutting feed)—approach significance, both with p values of 0.0515, suggesting they may play a role in CW behavior under certain conditions, though they fall just outside the typical 0.05 significance threshold. Voltage, however, does not show a statistically significant effect ($p = 0.2394$), either as a main factor or in its interactions. This indicates that within the studied range (55-65 V), voltage does not have a major influence on CW. Additionally, none of the quadratic terms were found to be statistically significant, although the quadratic term for Pulse Duration (D) (C^2) approaches significance ($p = 0.0546$), suggesting a possible nonlinear effect that may warrant further investigation.

$$\begin{aligned} \mathrm{CW} = & -1.02724 + (0.004911 \times V) + (0.021684 \times I) \\ & + (0.011508 \times D) + (0.029411 \times F) \\ & - (0.000050 \times V \times I) + (0.000035 \times V \times D) \\ & - (0.000237 \times V \times F) - (0.000105 \times I \times D) \\ & - (0.000237 \times I \times F) - (0.000031 \times D \times F) \\ & - (0.000047 \times V^2) - (0.000077 \times I^2) \\ & - (0.000037 \times D^2) + (0.000036 \times F^2) \end{aligned} \quad \text{(Eq 5)}$$

Equation 5 represents a quadratic regression model developed that incorporates linear, interaction, and quadratic effects of four machining parameters. Among the linear terms, all four parameters have positive coefficients, indicating that increases in these variables tend to widen the CW. Pulse interval ($0.021684 \times I$), pulse duration ($0.011508 \times D$), and cutting feed ($0.029411 \times F$) show relatively large and significant positive influences on CW. These findings align with the ANOVA results, which identified these three parameters as statistically significant contributors. In contrast, voltage ($0.004911 \times V$) also has a positive coefficient but was not found to be statistically significant, suggesting that changes in voltage have a weaker and more inconsistent effect on CW within the studied range. The interaction terms in the model capture the combined effects of two parameters being changed simultaneously. Most of these interactions have small negative coefficients; for example, voltage × pulse interval (−0.000050), pulse interval × pulse duration (−0.000105), and pulse duration × cutting feed (−0.000031). These negative coefficients indicate a synergistic effect, where the joint influence of increasing two parameters is less than the sum of their individual effects. Conversely, the interaction between voltage and pulse duration has a small positive coefficient (0.000035), suggesting a slight antagonistic effect. Importantly, the interaction between Pulse Interval (I) and Pulse Duration (D) (BC) was identified as significant in the ANOVA, and it exhibits a negative coefficient, reinforcing the idea of a non-additive and potentially beneficial interplay between these two parameters in minimizing CW. The quadratic terms in the model reflect nonlinear trends in the effect of each parameter on CW. The squared terms for voltage, pulse interval, and pulse duration all have negative coefficients, indicating downward curvature—meaning that CW increases with the parameter up to a point, after which it may start to level off or decrease slightly. Cutting feed shows a small positive quadratic coefficient ($0.000036 \times F^2$), suggesting a slight upward curvature in its effect. Although these trends hint at nonlinear behavior, none of the quadratic terms were statistically significant in the ANOVA, suggesting that the primary relationships between parameters and CW are predominantly linear within the investigated range.

Figure 9 illustrates the perturbation plot for CW; the red curve representing Pulse Duration (C) exhibits the steepest slope. This indicates that CW is most sensitive to changes in pulse duration around the reference point. As pulse duration increases beyond 120 μs, CW also increases significantly, suggesting a broader kerf. Conversely, reducing pulse duration sharply decreases the cut width, making it a critical factor for

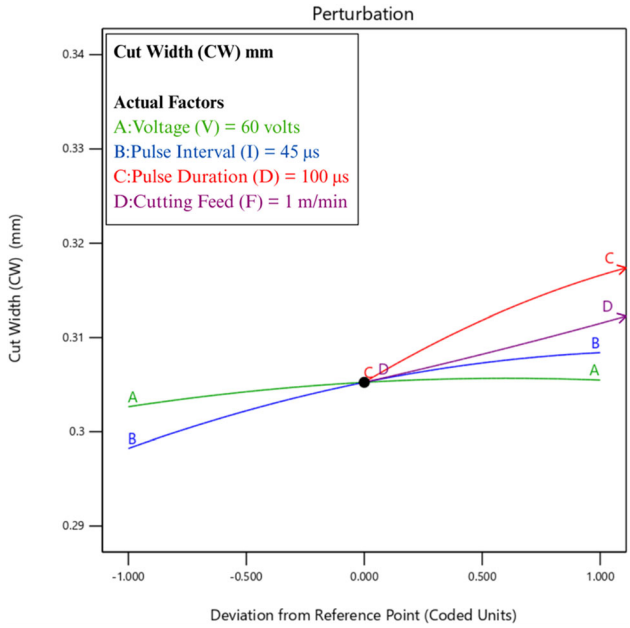

Fig. 9 Perturbation plot illustrating the sensitivity of CW

achieving precision cuts. This trend highlights the strong positive linear influence of pulse duration on CW and aligns with earlier ANOVA results, where pulse duration was found to be highly significant. The purple curve for Cutting Feed (D) also shows a pronounced upward slope. Increasing the cutting feed from the reference level leads to a noticeable increase in cut width, while reducing it results in a narrower kerf. This suggests a positive and significant relationship between cutting feed and CW, where lower feed rates are favorable for minimizing cut width. The response is not as steep as pulse duration's but is still notably influential, reaffirming cutting feed as a major parameter affecting CW. The blue curve, representing Pulse Interval (B), displays a moderate upward slope. This indicates a weaker, yet still positive, relationship with CW. Higher pulse interval values lead to slightly broader cuts, whereas reducing the interval contributes to a modest narrowing of the kerf (Ref 34). Although this effect is less pronounced than that of pulse duration or cutting feed, it remains meaningful within the studied parameter range. The green curve, corresponding to Voltage (A), remains relatively flat throughout the coded range. This suggests that voltage has a minimal effect on CW around the reference point of 60 volts. The model and ANOVA results confirm that voltage does not significantly influence CW, making it the least impactful among the four parameters in this region of the design space. The perturbation plot clearly identifies pulse duration as the dominant factor influencing CW, followed by cutting feed and pulse interval. Voltage exerts minimal influence within the studied range. Notably, the reference parameter combination (Voltage = 60 V, Pulse Interval = 45 μs, Pulse Duration = 100 μs, and Cutting Feed = 1 m/min) corresponds to the lowest observed CW of 0.305 mm (Run #8). To further minimize CW near this operating point, the plot suggests that reducing pulse duration would be the most effective single-variable adjustment.

Figure 10 comprises a series of three-dimensional response surface plots that visually illustrate the interactive effects of different pairs of Wire EDM parameters on CW. In Fig. 10(a), the interaction between voltage and pulse interval is examined while pulse duration is fixed at 110 μs and cutting feed at 5 m/min. The plot reveals that lower pulse interval values consistently produce narrower cuts across the voltage range. Voltage, in contrast, has a relatively minor effect, contributing to a slight increase in CW at higher values—especially when pulse interval is low. The surface suggests a mild interaction between these two parameters, with the predicted minimum CW located at the lower ends of both pulse interval and voltage.

Figure 10(b) explores the effect of voltage and pulse duration, holding the pulse interval at 45 μs and cutting the feed at 5 m/min. Here, pulse duration exerts a clear influence: shorter durations lead to narrower cuts. Voltage again shows a limited impact, with a slight increase in CW as voltage increases. A mild interaction is noted, where the widening effect of longer pulse duration is slightly amplified at higher voltage levels. The narrowest kerf (CW) in this scenario is achieved with low pulse duration and low voltage. In Fig. 10(c), the relationship between voltage and cutting feed is shown, with the pulse interval set at 45 μs and the pulse duration at 110 μs. The CW is notably sensitive to cutting feed: increasing the feed rate leads to a broader kerf, while decreasing it results in a narrower cut. Voltage, once more, contributes minimally to CW changes, with a subtle increase at higher levels. The surface suggests a relatively simple interaction, with the optimal (minimum) CW achieved at low values of both parameters. Figure 10(d) investigates the combined effect of pulse interval and pulse duration, with voltage fixed at 59 volts and cutting feed at 5 m/min. Both parameters significantly influence CW, with lower values yielding narrower cuts. The plot shows a strong interaction: the positive effect of increasing pulse duration on CW becomes more pronounced at higher pulse interval settings. The predicted minimum CW lies in the region where both parameters are minimized, underscoring their critical roles in controlling kerf width. In Fig. 10(e), the interaction between pulse interval and cutting feed is shown, while voltage is held at 59 volts and pulse duration at 110 μs. Both parameters exhibit a strong positive influence on CW—higher values result in wider cuts. A clear interaction is present, where the increase in CW due to pulse interval is more substantial at higher cutting feed values. The surface indicates that the narrowest kerf occurs when both pulse interval and cutting feed are set to their lowest levels.

Figure 10(f) focuses on the relationship between pulse duration and cutting feed, with fixed values of voltage (59 volts) and pulse interval (45 μs). Both parameters individually contribute to increased CW, and their combination exhibits a positive but relatively less complex interaction compared to other pairings. The CW increases consistently with higher values of either parameter. The optimal narrow kerf is achieved at the lower ends of both pulse duration and cutting feed. These plots serve as valuable tools for selecting optimal parameter settings to minimize CW and improve dimensional precision in the machining of X5CrNi18-10 ASS.

3.4 Multi-criteria Optimization

In manufacturing processes such as Wire EDM, optimizing performance involves balancing multiple, often conflicting, output criteria. For instance, maximizing the CR improves productivity, but it may come at the expense of Ra or CW, which are critical for surface integrity and dimensional accuracy. Multi-criteria optimization provides a systematic framework for resolving such trade-offs by identifying process parameter settings that offer the best compromise among all desired outcomes. In this study, RSM, combined with a desirability framework, is employed to optimize the Wire EDM process parameters—voltage, pulse interval, pulse duration, and cutting feed—with respect to the three key responses.

Figure 11 presents a desirability plot corresponding to Solution 1 from a set of 80 optimization results generated using the desirability function approach within the framework of RSM. For Solution 1, all four input parameters achieved individual desirability scores of 1.0. This implies that the selected levels of these process parameters lie within the optimal or most acceptable range based on the constraints or preferences set during optimization. It also suggests that the optimization focused on meeting performance targets for the output responses, rather than constraining the input settings to specific values. Among the response variables, Ra achieved a desirability of approximately 0.953, indicating that the predicted surface finish is very close to the desired target—likely set to minimize Ra for improved surface quality. CW followed closely with a desirability value around 0.915, suggesting the predicted kerf width is near the optimal range—probably aimed at minimizing CW for dimensional accuracy and precision. Meanwhile, CR achieved a slightly lower desirability of about 0.844, which still reflects a favorable result but implies that the

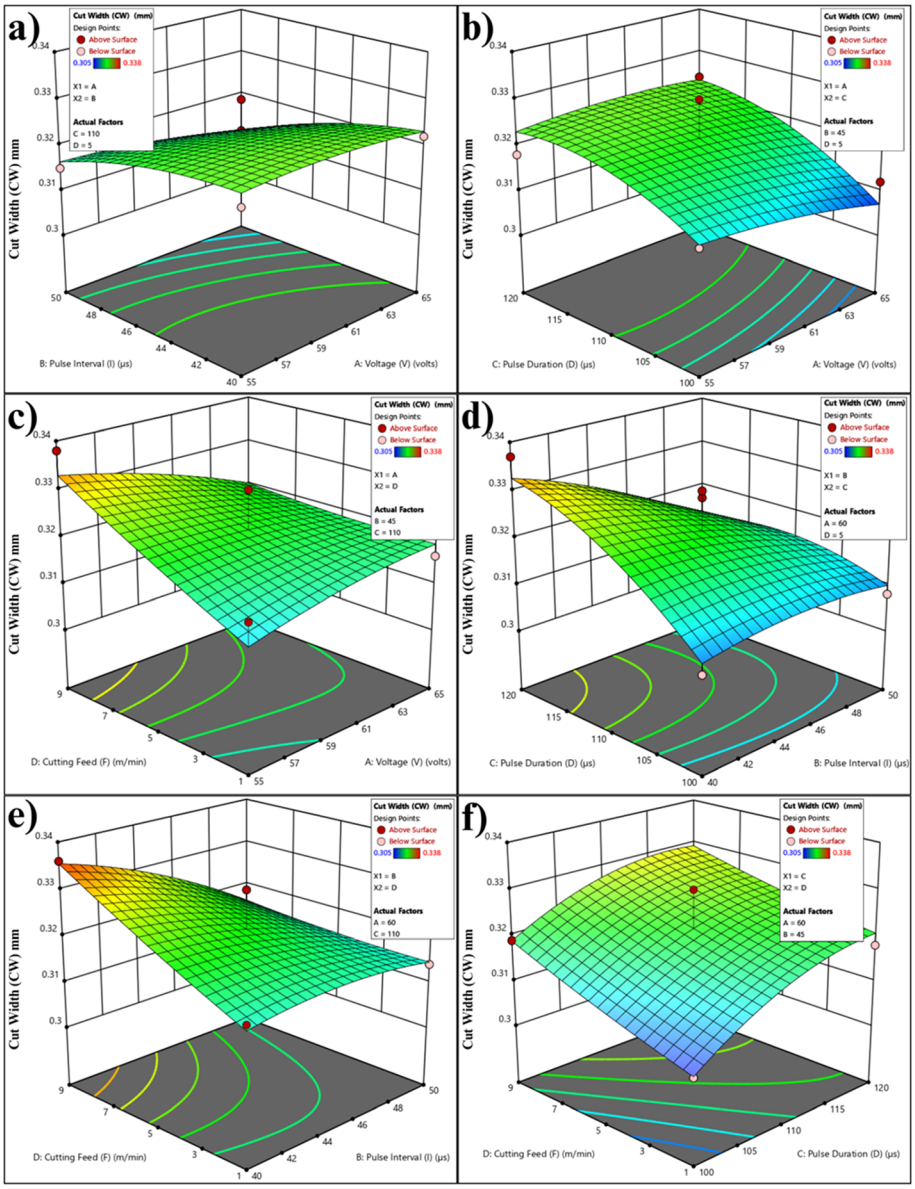

Fig. 10 3D response surface plots showing the interactive effects of parameter pairs on CW: (a) Voltage and Pulse Interval, (b) Voltage and Pulse Duration, (c) Voltage and Cutting Feed, (d) Pulse Interval and Pulse Duration, (e) Pulse Interval and Cutting Feed, and (f) Pulse Duration and Cutting Feed

predicted cutting rate is not fully at the optimal level—possibly due to the trade-off with surface quality and dimensional control. The combined desirability for this solution is approximately 0.903, signifying a high-quality compromise among the competing objectives. A value close to 1 reflects that the solution offers a strong overall balance, successfully navigating the trade-offs between maximizing CR and minimizing surface roughness and cut width. This makes Solution 1 a well-rounded choice for practitioners seeking to enhance productivity while maintaining high-quality machining outcomes in the Wire EDM of X5CrNi18-10 ASS.

Figure 12 presents a series of cube plots that offer a three-dimensional visualization of the design space and the corresponding predicted responses (Desirability, CR, Ra, and CW) within the experimental domain of the Wire EDM process. These plots illustrate the effect of the three key process variables: Voltage (A: 55-65 V), Pulse Interval (B: 40-50 μs), and Pulse Duration (C: 100-120 μs). In these visualizations, cutting feed is held constant at an optimized level, although its exact value is not explicitly provided. Each cube displays the response values at the eight corners defined by the low and high levels of the three factors and marks the predicted optimal solution within the space. The desirability cube reveals the overall desirability values for each parameter combination, ranging from 0.000 to 0.903. A desirability value of 0.903 at a specific parameter combination highlights the location of the predicted optimal solution, where the trade-offs among multiple performance objectives (high CR, low Ra, and low CW) are most effectively balanced. This plot serves as a high-level synthesis of the other cubes, pointing to the most favorable region in the parameter space for simultaneously optimizing all target responses. The CR Cube illustrates how material removal rate varies across the design space. Predicted CR values range from 28.6 to 50.9 mm^3/min, indicating a substantial effect of

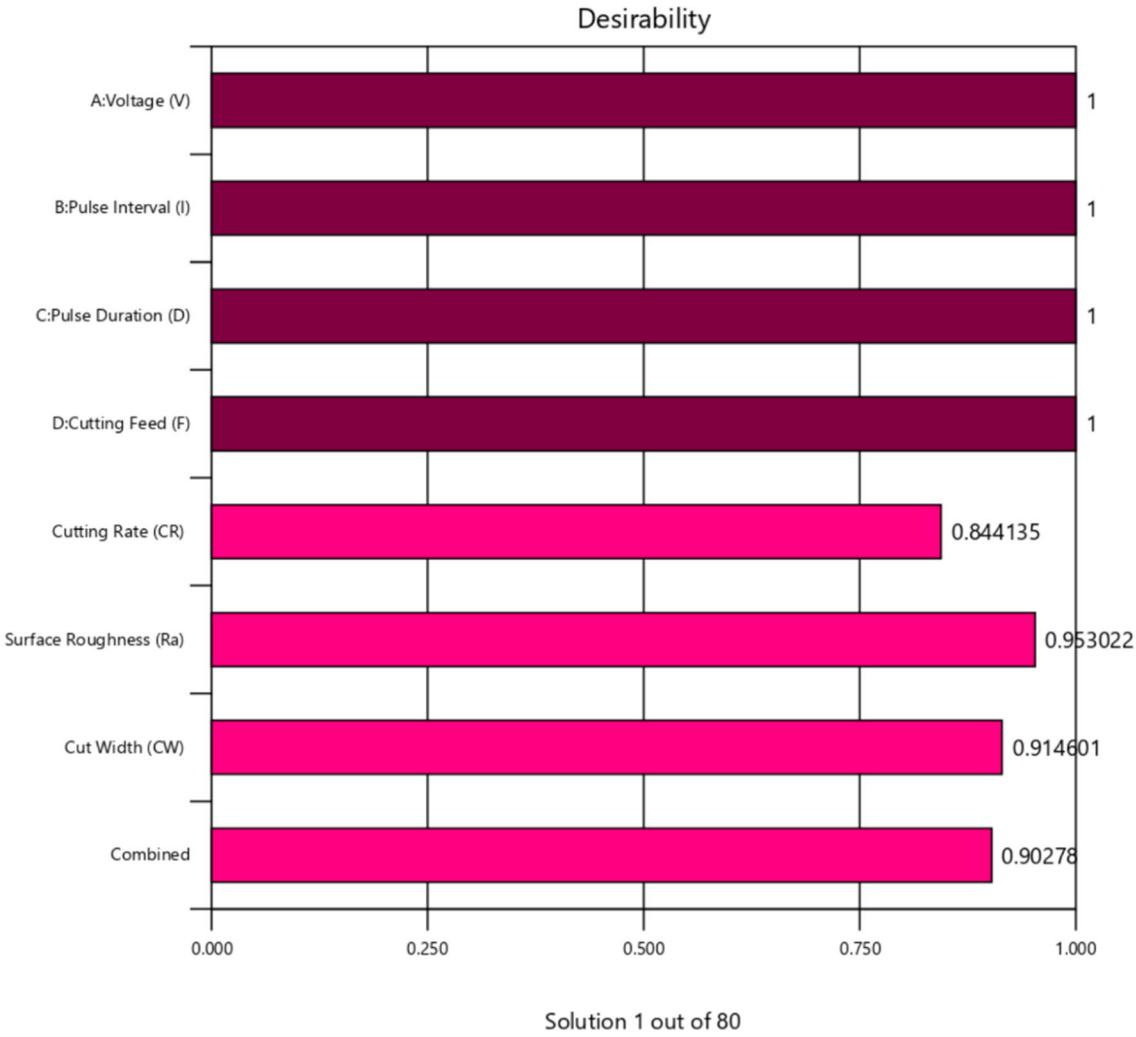

Fig. 11 Desirability plot for the optimal multi-response solution

the input parameters. Higher CR values are generally associated with higher voltage and pulse duration, suggesting these parameters positively contribute to material removal efficiency. The predicted optimal solution in this cube corresponds to a CR of 40.441 mm^3/min, reflecting a reasonable trade-off between speed and quality.

In the Ra cube, predicted Ra values range from approximately −0.103 to 5.616 μm. The presence of negative Ra values at some parameter combinations likely reflects extrapolation errors or model limitations at the design space extremes, reinforcing the need to operate within the experimentally validated region. The optimal solution corresponds to an Ra of 0.806 μm, which indicates a relatively smooth surface finish. Lower Ra values are typically achieved at lower pulse duration levels, in conjunction with specific voltage and pulse interval settings. The CW cube presents a narrower range of predicted values, from 0.303 to 0.344 mm, showing that this response is less sensitive to parameter changes compared to CR or Ra. A CW of 0.313 mm is observed at the predicted optimal condition, representing a desirable narrow cut width. The narrowest cuts tend to be associated with lower pulse duration and carefully selected combinations of voltage and pulse interval.

Figure 13 illustrates the optimization profile derived from the desirability function approach for the Wire EDM of the X5CrNi18-10 ASS. The optimization results suggest the following optimal combination of process parameters. Voltage (V) is set at 65 volts, which is the upper boundary of the investigated range. This setting, indicated by the red flag, may have reached a limiting point within the current design space. Pulse Interval (I) is optimized at approximately 45.4879 μs, a mid-range value selected to balance its influence on all responses. Pulse Duration (D) is set at approximately 103.571 μs, indicating that moderate energy input leads to improved performance. Cutting Feed (F) is optimized at 8.93676 m/min, again very close to the upper end of the studied range, implying a strong positive contribution to performance. The use of red flags for voltage and cutting feed, both positioned at the upper bounds, suggests the potential for improved performance beyond these levels, although this lies outside the limits of the current experimental design.

At the optimized parameter combination, the predicted outcomes for the key machining responses are as follows: predicted at 40.441 mm^3/min, indicating a high cutting rate and thus enhanced productivity. The CR response curve reflects a rising trend with increasing voltage and cutting feed, predicted

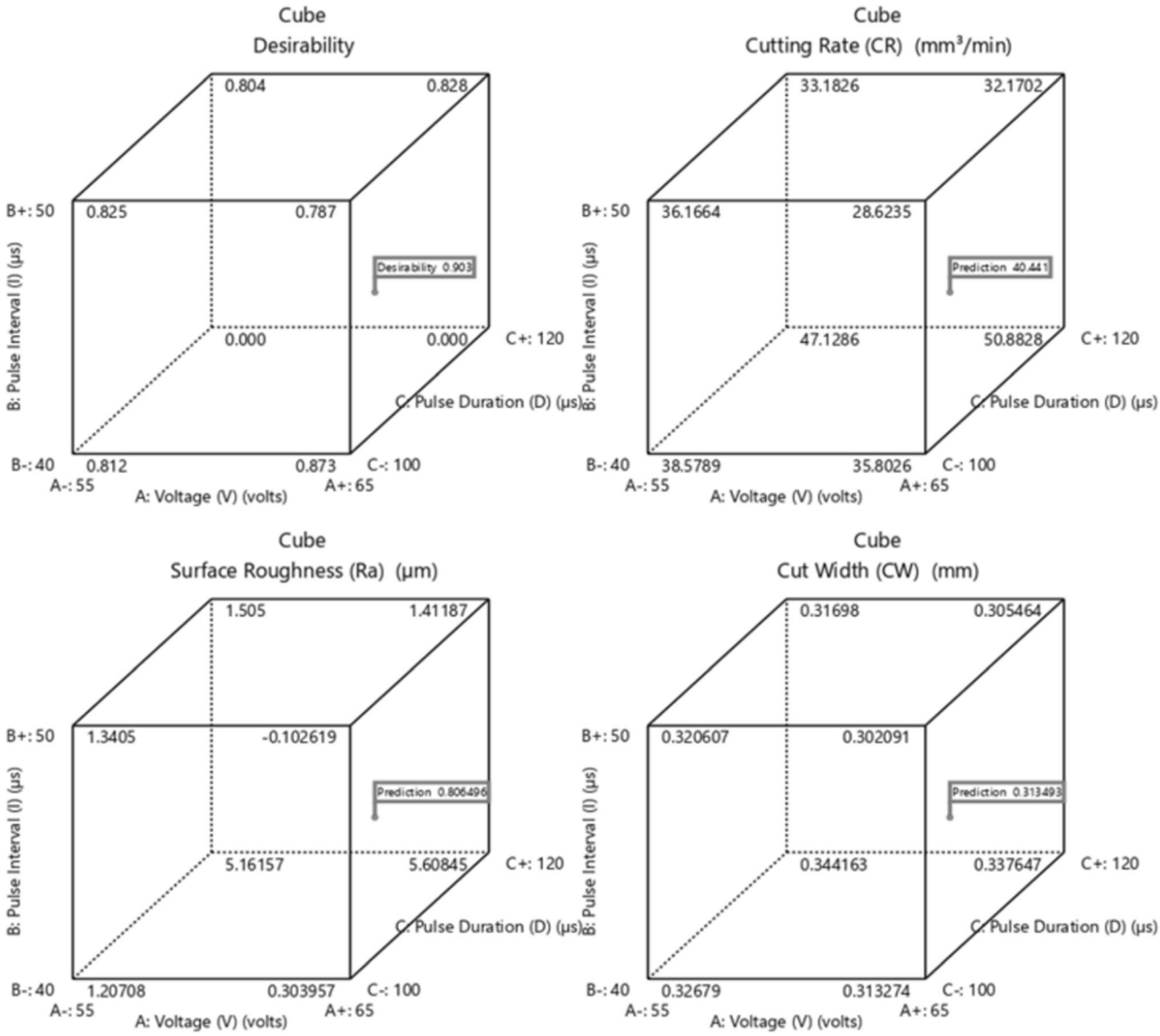

Fig. 12 Cube plots visualizing the variation of Desirability, CR, Ra, and CW

at 0.8065 μm, signifying a smooth surface finish. Lower pulse duration and moderate pulse interval are critical to achieving this level of surface quality. The predicted value of 0.3135 mm indicates a relatively narrow kerf, which is desirable for achieving dimensional accuracy. The influence of pulse duration and cutting feed is evident in achieving this reduced CW. Each response curve in the profile illustrates how the corresponding response changes with variations in a single factor while keeping others fixed at their optimal settings. These visual trends aid in understanding the sensitivity of each response to parameter adjustments. The combined desirability score achieved at these optimal settings is 0.903, which is very close to the ideal value of 1. This score signifies that the chosen parameter configuration effectively satisfies the multiple, and sometimes conflicting, objectives of the Wire EDM process. It identifies that operating at higher voltage and cutting feed enhances material removal, while carefully tuned pulse interval and pulse duration are essential for minimizing surface roughness and cut width (Ref 35). The profile confirms that optimal performance is not achieved by maximizing or minimizing each parameter independently, but rather through a nuanced combination that leverages the interactions between factors.

3.5 Validation Experiment

Table 7 presents the outcomes of a validation experiment aimed at verifying the accuracy of the optimal response values predicted by the RSM model in the context of Wire EDM of X5CrNi18-10 ASS. The validation experiment employed the optimized parameter settings derived from the desirability analysis: Voltage (V): 65 volts, Pulse Interval (I): 45.4879 (45) μs, Pulse Duration (D): 103.571 (105) μs, and Cutting Feed (F): 8.93676 (9) m/min (rounded values for machining). These values represent the combination that was predicted to yield a high cutting rate, minimal surface roughness, and a narrow cut width. The experimental result shows a slightly higher cutting rate (41.729 mm^3/min) than predicted (40.441 mm^3/min), with a small deviation of 3.18%. This close match suggests that the

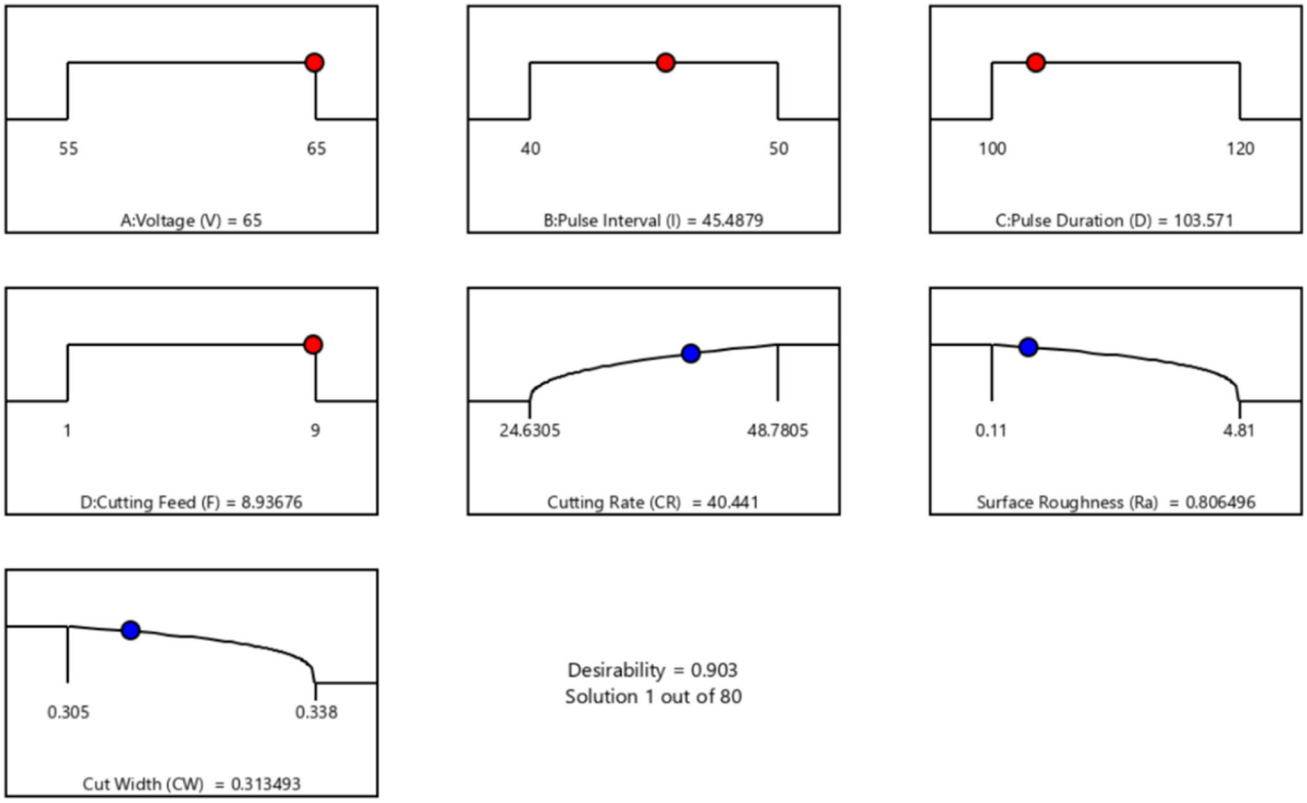

Fig. 13 Optimization profile showing the effect of each parameter on individual responses and the composite desirability

Table 7 Validation experiment results: comparison between predicted and experimental response values

	Machining Parameter				Response Parameter		
	Voltage (V)	Pulse Interval (I)	Pulse Duration (D)	Cutting Feed (F)	Cutting Rate (CR)	Surface Roughness (Ra)	Cut Width (CW)
Prediction	65 volts	45.4879 μs	103.571 μs	8.93676 m/min	40.441 mm^3/min	0.806496 μm	0.313493 mm
Experimentation					41.729 mm^3/min	1.03 μm	0.315 mm
Deviation (%)					3.18	27.72	0.48

RSM model accurately captures the relationship between the input parameters and material removal rate under the given conditions. The Ra shows a larger deviation, with the experimental value (1.03 μm) significantly higher than the model prediction (≈0.8065 μm). This 27.72% deviation indicates that the model may have under-predicted the surface finish quality, potentially due to unmodeled factors or limitations in the quadratic model's ability to represent the surface finish behavior under the tested conditions. For CW, the experimental (0.315 mm) and predicted (≈0.3135 mm) values are nearly identical, with a very small deviation of 0.48%. This strong agreement confirms the model's high accuracy in predicting cut width, reinforcing its robustness when controlling dimensional accuracy. The validation experiment confirms the reliability and accuracy of the developed RSM models, particularly for predicting cutting rate and cut width, which both showed minimal deviation from the actual experimental values. These results indicate that the optimization process successfully identified parameter settings that deliver high performance in terms of productivity and dimensional control.

Figure 14 presents SEM images that offer a microstructural comparison of the surfaces of X5CrNi18-10 ASS machined using Wire EDM under two different sets of conditions: (a) parameters that yielded the maximum CR, and (b) optimized conditions that balanced CR with Ra and CW. Figure 14(a) shows the surface produced under the machining conditions that achieved the highest observed CR of 48.7805 mm^3/min (Voltage = 60 V, Pulse Interval = 45 μs, Pulse Duration = 120 μs, Cutting Feed = 9 m/min) (Run #3). This surface is marked by deep and irregular craters, resulting from intense localized melting and vaporization caused by high-energy discharges. The longer pulse duration and high cutting feed rate used in this run likely contributed to more energetic spark events, which aggressively removed material and left behind larger molten zones (Ref 36). The image also shows substantial re-solidified material, evident in the form of globular and uneven surface deposits. These are remnants of molten material that were ejected and then re-solidified on the surface, increasing the roughness. Additionally, adhered debris and particles, possibly from both the workpiece and the eroded tool

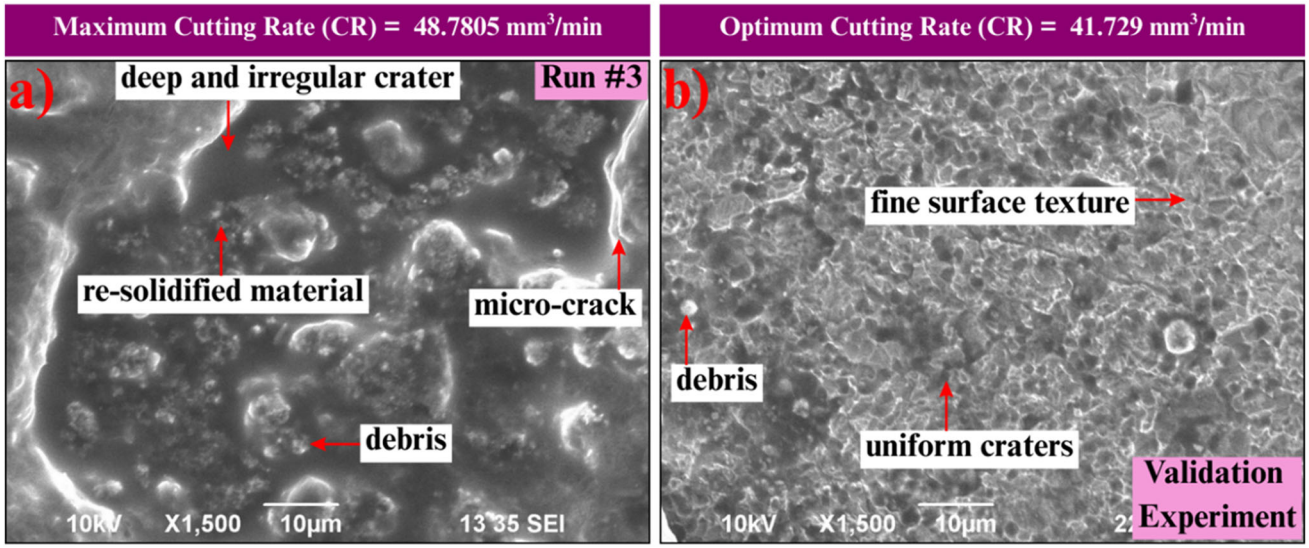

Fig. 14 SEM images comparing surface morphology: (a) machined at maximum CR conditions, and (b) machined at optimized multi-response conditions

electrode, are visible. This accumulation is likely due to insufficient flushing efficiency under high MRR conditions. Signs of micro-cracks and voids can also be observed, which may have developed due to thermal stresses from rapid heating and cooling cycles inherent to Wire EDM at high-energy settings. Overall, the surface exhibits a rough and irregular morphology, characteristic of high-speed erosion dominated by aggressive sparking.

In contrast, Fig. 14(b) shows the surface obtained under the optimized machining parameters used during the validation experiment (Voltage = 65 V, Pulse Interval = 45 μs, Pulse Duration = 103 μs, and Cutting Feed = 9 m/min), which resulted in a cutting rate of 41.729 mm^3/min. Although slightly lower than the maximum CR, this condition was chosen for its balanced performance across all key responses. The surface in this image appears smoother and more refined, with shallower and more uniform craters. These features suggest a more stable and controlled erosion process. The pulse duration and energy input are more moderate compared to Run #3, resulting in less aggressive melting. The amount of re-solidified material is noticeably reduced, and the presence of adhered debris is minimal, indicating more efficient flushing and cleaner spark conditions. The overall surface texture is finer, reflecting the effectiveness of the optimization strategy in minimizing surface roughness without significantly sacrificing productivity. The distinct differences in surface topography between the two images can be directly linked to the spark energy and thermal effects associated with each machining condition. In Run #3, the high pulse duration and feed rate increased the spark energy and material removal rate, but at the cost of greater thermal damage, leading to rougher textures and deeper craters. The higher material ejection also caused more re-solidification and debris accumulation on the surface. In the optimized condition, a balanced discharge energy was achieved by slightly increasing voltage and reducing pulse duration, allowing for more controlled spark behavior. This resulted in better surface integrity with fewer thermal defects, reduced molten material deposition, and enhanced surface finish. The SEM analysis effectively demonstrates the trade-off between maximum material removal and surface quality in the Wire EDM process. While aggressive settings like those in Run #3 lead to higher productivity, they compromise surface integrity due to intense thermal effects. In contrast, the optimized parameters derived from multi-criteria analysis provide a well-balanced outcome, producing smoother surfaces with more uniform features while still maintaining a high cutting rate.

Figure 15 presents profilometric surface roughness profiles for X5CrNi18-10 ASS machined using Wire EDM under two different parameter settings: (a) conditions that resulted in the maximum Ra observed during the experimental runs, and (b) the optimized conditions identified through RSM that aim to balance surface finish, cutting rate, and dimensional accuracy. The surface profile depicted in Fig. 15(a) corresponds to Run #15, which produced the highest Ra value of 4.81 μm. This profile shows pronounced vertical deviations, with deep valleys and sharp peaks spanning a vertical scale of 120 μm. The irregularity and steepness of these features reflect a highly uneven erosion process, likely caused by unstable spark discharges or excessive localized melting. The surface also exhibits long-wavelength undulations, indicating roughness over extended lengths of the workpiece. These irregularities suggest that the machining parameters used in Run #15—namely, Voltage = 60 V, Pulse Interval = 40 μs, Pulse Duration = 120 μs, and a notably low Cutting Feed of 5 m/min—contributed to poor surface integrity. The moderate feed rate may have led to localized overheating and inefficient flushing of debris, which in turn promoted secondary discharges and material redeposition, exacerbating surface roughness (Ref 37).

Figure 15(b) shows the surface profile obtained under the optimized parameter settings used in the validation experiment, which achieved a significantly lower Ra value of 1.03 μm. The profile spans a vertical range of only 15 μm, and the surface deviations are much smaller and more uniform compared to Fig. 15(a). The peaks and valleys appear smoother and more rounded, suggesting a stable and consistent material removal process. This improved surface finish was achieved using Voltage = 65 V, Pulse Interval = 45.49 μs, Pulse Duration = 103.57 μs, and Cutting Feed = 8.94 m/min. These settings likely promoted controlled energy delivery per discharge,

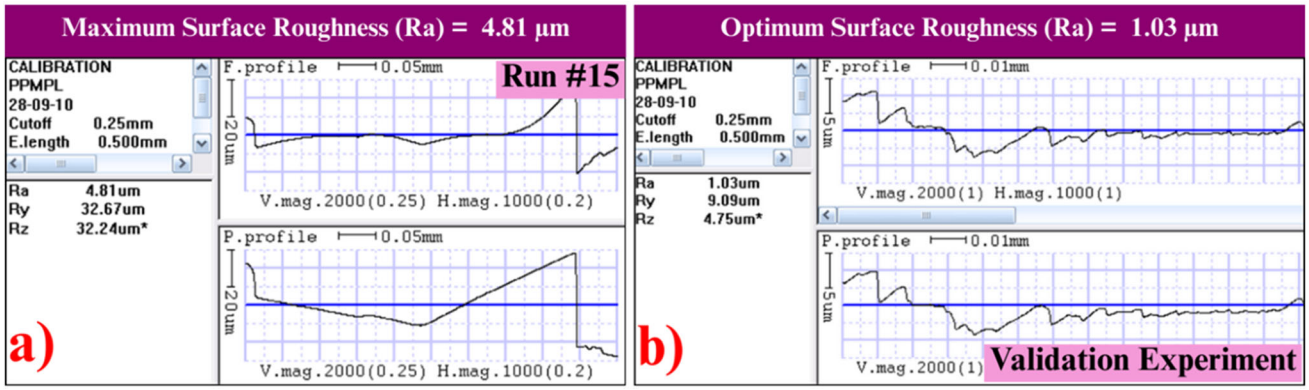

Fig. 15 Surface roughness profiles: (a) obtained at maximum Ra conditions, and (b) obtained at optimized multi-response conditions

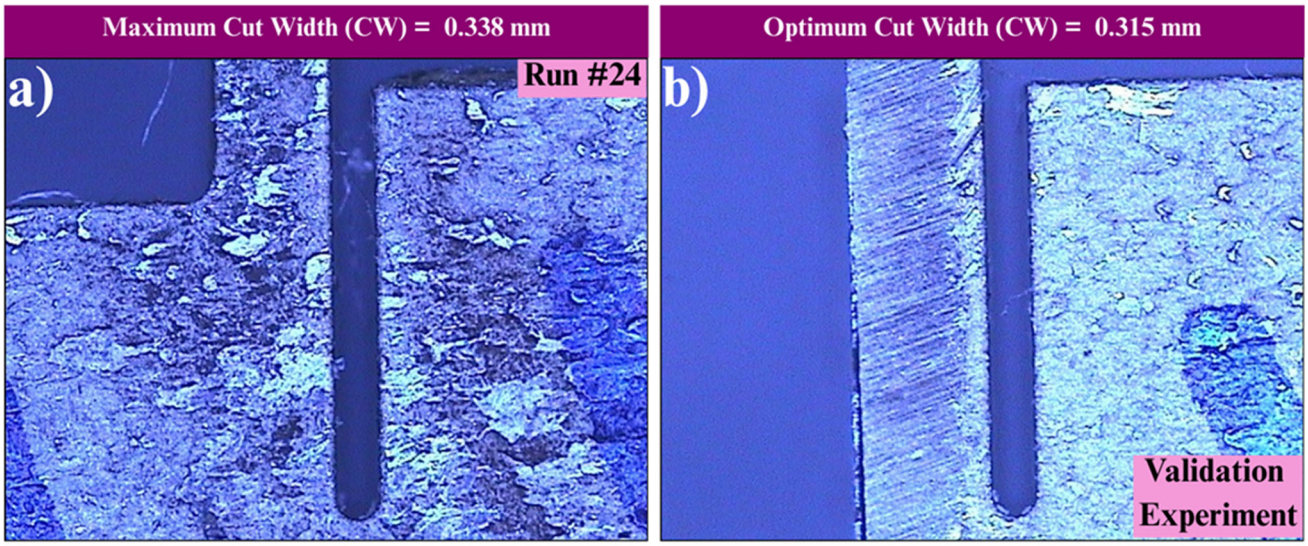

Fig. 16 Video measuring system images: (a) maximum CW condition, and (b) optimized multi-response condition

efficient debris removal, and minimal re-solidification on the machined surface. As a result, the profile is characterized by shorter-wavelength, finer-texture features, indicative of an improved machining environment and surface quality. The stark contrast between the two surface roughness profiles can be attributed to several interrelated factors associated with the Wire EDM parameters. Run #15 likely experienced unstable or overly energetic discharges due to its moderate cutting feed and moderate pulse duration, resulting in uncontrolled material removal and re-solidification. In contrast, the optimized parameters provided a balanced spark energy, leading to consistent erosion and smoother surfaces. The moderate cutting feed in Run #15 may have allowed more heat to accumulate in localized regions, causing deeper craters and poor flushing. The higher feed rate in the optimized condition enabled faster removal of material and better cooling, which helped minimize surface irregularities. Poor flushing conditions at moderate cutting feed increase the likelihood of secondary discharges and molten material redeposition, both of which elevate surface roughness. The optimized setup likely improved dielectric flow and debris clearance, leading to fewer surface defects and finer textures.

Figure 16 presents visual comparisons of the machined slots in X5CrNi18-10 ASS produced under two distinct Wire EDM conditions. Two conditions are considered: (a) machining parameters that yielded the maximum CW observed during the experiments (Run #24), and (b) the optimized conditions identified via multi-objective optimization and used for the validation experiment. Figure 16(a) corresponds to Run #24, which produced the widest slot with a measured CW of 0.338 mm—the highest value recorded during the study. The cut is visibly broader, aligning with the quantitative CW measurement. The slot edges appear somewhat uneven and rough, suggesting variability in spark intensity or instability in material removal during the process. Such irregularities are often a result of inconsistent energy delivery or inadequate flushing of molten debris. The surface texture within the kerf also appears coarse and uneven, indicative of less controlled machining conditions. The machining parameters used in Run #24 included Voltage = 55 V, Pulse Interval = 45 μs, Pulse Duration = 110 μs, and Cutting Feed = 9 m/min. This particular combination likely generated larger spark gaps and more aggressive material removal per discharge, which contributed to the increased kerf width. The relatively short pulse interval and

moderate feed may have also induced thermal instabilities, exacerbating kerf variability.

In contrast, Fig. 16(b) illustrates the machined slot obtained under optimized parameter settings derived from the RSM-based optimization. The measured CW is 0.315 mm, significantly narrower than that of Run #24. The slot width is visibly reduced, confirming the improved dimensional control under the optimized conditions. The kerf boundaries are cleaner and more uniform, suggesting a more stable and precise material removal process. The texture inside the cut appears finer and more refined, indicating enhanced surface integrity and better control over thermal energy. These results were achieved using Voltage = 65 V, Pulse Interval = 45 μs, Pulse Duration = 103 μs, and Cutting Feed = 9 m/min (rounded values for machining). These optimized parameters provided a more balanced energy input, allowing for efficient cutting with reduced side erosion and minimal spark dispersion, ultimately resulting in a narrower and cleaner kerf. The clear differences in slot width and quality between the two conditions can be attributed to several core aspects of the Wire EDM process. In Wire EDM, the spark gap determines how far the wire electrode can be from the material before electrical discharge occurs. A larger effective gap, such as that created under Run #24 conditions, leads to a wider kerf. Conversely, the optimized settings allow for tighter control over this gap, resulting in a narrower cut. The combination of voltage, pulse interval, and pulse duration governs the energy transferred in each discharge. High-energy, prolonged discharges can erode more material, causing kerf expansion. The optimized parameters ensured a more consistent and moderate energy input, reducing excessive side wear. The cutting feed rate also affects cut precision. While low feed rates may reduce cutting speed, they can lead to thermal accumulation and kerf widening. The higher feed used in the optimized case likely enabled more efficient debris removal and thermal regulation, improving dimensional accuracy (Ref 38). The comparative images in Fig. 16 clearly illustrate the impact of machining parameters on CW and kerf quality in the Wire EDM for X5CrNi18-10 ASS. Under parameters aimed at maximizing CW, the resulting slot is wider, less uniform, and exhibits a rougher internal surface. In contrast, the optimized conditions produce a narrower, more consistent kerf with a smoother finish, reflecting improved dimensional accuracy and machining control.

4. Conclusions

This study successfully applied Response Surface Methodology (RSM) using a Box–Behnken Design to model and optimize the Wire EDM process for X5CrNi18-10 austenitic stainless steel. The key takeaways are as follows:

- Quadratic models were developed for cutting rate (CR), surface roughness (Ra), and cut width (CW). ANOVA results highlighted pulse duration and cutting feed as the most influential factors across all three responses. The model for CR showed strong predictive accuracy, while the Ra model exhibited a significant lack of fit, suggesting the need for further refinement in predicting surface finish.
- A multi-objective optimization using the desirability function led to an optimal set of process parameters: Voltage = 65 V, Pulse Interval = 45.49 μs, Pulse Duration = 103.57 μs, and Cutting Feed = 8.94 m/min. This parameter combination achieved a high overall desirability score of 0.903, effectively balancing the trade-off between machining speed and surface quality.
- Validation experiments confirmed the robustness of the developed models. Predictions closely matched experimental results for CR (3.18% deviation) and CW (0.48% deviation). However, Ra showed a larger deviation (27.72%), reflecting the inherent difficulty in modeling surface roughness and reinforcing the model's identified lack of fit.
- SEM imaging and surface profilometry confirmed the success of the optimized settings. Compared to high-CR conditions, the optimized parameters resulted in a much smoother surface, characterized by shallower craters, less re-deposited material, and improved surface texture, indicating a better balance between performance and quality.

The RSM-based optimization approach proved effective in identifying a practical and high-performance set of parameters for Wire EDM of X5CrNi18-10 stainless steel. The optimized process enhances productivity while maintaining dimensional accuracy and significantly improving surface integrity, making it a strong candidate for precision applications.

References

1. L. Slătineanu, O. Dodun, M. Coteaţă, G. Nagîţ, I.B. Băncescu, and A. Hriţuc, Wire Electrical Discharge Machining—A Review, *Machines*, 2020, **8**(4), p 69. https://doi.org/10.3390/machines8040069
2. S.N. Vijayan, C. Samson Jerold Samuel, and A. Saiyathibrahim, Unlocking the Potential of WEDM for LM26 Hybrid Composites: Multi-Objective Optimization Using RSM and Desirability Approach, *Phys. Scr.*, 2025, **100**(5), p 055019. https://doi.org/10.1088/1402-4896/adce4b
3. R. Ranganathan, A. Saiyathibrahim, R. Velu, V.S. Jatti, D.G. Mohan, and P. Vijayakumar, Achieving Multi-Response Optimization of Control Parameters for Wire-EDM on Additive Manufactured AlSi10Mg Alloy Using Taguchi-Grey Relational Theory, *Eng. Res. Express*, 2025, **7**(1), 015404. https://doi.org/10.1088/2631-8695/ada225
4. C. Sarala Rubi, J.U. Prakash, S.J. Juliyana, R. Čep, S. Salunkhe, K. Kouril, and S. Ramdas Gawade, Comprehensive Review on Wire Electrical Discharge Machining: A Non-Traditional Material Removal Process, *Front. Mech. Eng.*, 2024, **10**, p 1322605. https://doi.org/10.3389/fmech.2024.1322605
5. A. Weiß, H. Gutte, and J. Mola, Contributions of ε and α′ TRIP Effects to the Strength and Ductility of AISI 304 (X5CrNi18-10) Austenitic Stainless Steel, *Metall. Mater. Trans. A Phys. Metall. Mater. Sci.*, 2016, **47**, p 112–122. https://doi.org/10.1007/s11661-014-2726-y
6. N. Sagathiya, M. Singh, V. Sharma, and J. Ramkumar, Performance Comparison of Wire-Electrochemical Machining and Wire-Electrical Discharge Machining for the Processing of Stainless Steel-304, *J. Mater. Eng. Perform.*, 2025 https://doi.org/10.1007/s11665-025-11199-1
7. D. Pendokhare and S. Chakraborty, A Review on Multi-objective Optimization Techniques of Wire Electrical Discharge Machining, *Arch. Comput. Methods Eng.*, 2024, **32**, p 1797–1839. https://doi.org/10.1007/s11831-024-10195-3
8. K. Lal and R. Trehan, Review of Wire Breakage Causes and Mitigation Strategies in Wire Electrical Discharge Machining, *Mach. Sci. Technol.*, 2025, **29**(2), p 212–258. https://doi.org/10.1080/10910344.2025.2475463
9. N. Vijayakumar and J. Chandradass, Optimizing Wire Electrical Discharge Machining Parameters for Enhanced Gear Machining Performance: A Machine Learning Approach on 20MnCr5 Steel, *J.*

Mater. Eng. Perform., 2024 https://doi.org/10.1007/s11665-024-10131-3
10. K. Lingadurai, B. Nagasivamuni, M. Muthu Kamatchi, and J. Palavesam, Selection of Wire Electrical Discharge Machining Process Parameters on Stainless Steel AISI Grade-304 Using Design of Experiments Approach, *J. Inst. Eng. India Ser. C*, 2012, **93**, p 163–170. https://doi.org/10.1007/s40032-012-0020-6
11. G.H. Gowd, M.G. Reddy, B. Sreenivasulu, and M. Ravuri, Multi Objective Optimization of Process Parameters in WEDM During Machining of SS304, *Procedia Mater. Sci.*, 2014, **5**, p 1408–1416. https://doi.org/10.1016/j.mspro.2014.07.45
12. A.A. Azawqari, M.A. Amrani, L. Hezam, M. Baggash, and Z.Z. Abidin, Multi-objectives Optimization of WEDM Parameters on Machining of AISI 304 Based on Taguchi Method, *Int. J. Adv. Manuf. Technol.*, 2024, **134**(11), p 5493–5510. https://doi.org/10.1007/s00170-024-14423-9
13. B. Mathew, B.A. Benkim, and J. Babu, Multiple Process Parameter Optimization of WEDM on AISI304 Using Utility Approach, *Procedia Mater. Sci.*, 2014, **5**, p 1863–1872. https://doi.org/10.1016/j.mspro.2014.07.494
14. N. Naeim, M.A. AbouEleaz, and A. Elkaseer, Experimental investigation of Surface Roughness and Material Removal Rate in Wire EDM of Stainless Steel 304, *Materials*, 2023, **16**(3), p 1022. https://doi.org/10.3390/ma16031022
15. K. Ishfaq, N. Ahmad, M. Jawad, M.A. Ali, and A. M. Al-Ahmari, Evaluating Material's Interaction in Wire Electrical Discharge Machining of Stainless Steel (304) for Simultaneous Optimization of Conflicting Responses, *Materials*, 2019, **12**(12), 1940. https://doi.org/10.3390/ma12121940
16. N.J. Rathod, P. Bonde, and H.R. Nehete, Parametric Optimization of WEDM of SS 304 Stainless Steel for Material Removal Rate and Surface Roughness Using Taguchi and Response Surface Methodology, *Interactions*, 2025, **246**(1), p 60. https://doi.org/10.1007/s10751-025-02273-0
17. S. Seshaiah, D. Sampathkumar, M. Mariappan, A. Mohankumar, G. Balachandran, M. Kaliyamoorthy, and R. Gopal, Optimization on Material Removal Rate and Surface Roughness of Stainless Steel 304 Wire Cut EDM by Response Surface Methodology, *Adv. Mater. Sci. Eng.*, 2022, **2022**(1), p 6022550. https://doi.org/10.1155/2022/6022550
18. T. Chaudhary, A.N. Siddiquee, and A.K. Chanda, Effect of Wire Tension on Different Output Responses During Wire Electric Discharge Machining on AISI 304 Stainless Steel, *Defence Technol.*, 2019, **15**(4), p 541–544. https://doi.org/10.1016/j.dt.2018.11.003
19. D. Srinivasan, N. Ganesh, H. Ramakrishnan, R. Balasundaram, R. Sanjeevi, and M. Chandran, Investigation of Surface Roughness and Material Removal Rate of WEDM of SS304 Using ANOVA and Regression Models, *Surf. Topogr. Metrol. Prop.*, 2022, **10**(2), 025014. https://doi.org/10.1088/2051-672X/ac6c9e
20. Z.A. Khan, A.N. Siddiquee, N.Z. Khan, U. Khan, and G.A. Quadir, Multi Response Optimization of Wire Electrical Discharge Machining Process Parameters Using Taguchi Based Grey Relational Analysis, *Procedia Mater. Sci.*, 2014, **6**, p 1683–1695. https://doi.org/10.1016/j.mspro.2014.07.154
21. M. Natarajan, T. Pasupuleti, R. Silambarasan, and L.N. Katta, Development of Prediction Models for Spark Erosion Machining of SS304 Using Regression Analysis (No. 2022-28-0339). SAE Technical Paper, 2022. https://doi.org/10.4271/2022-28-0339
22. S.A. El-Bahloul, Optimization of Wire Electrical Discharge Machining Using Statistical Methods Coupled with Artificial Intelligence Techniques and Soft Computing, *SN Appl. Sci.*, 2020, **2**, p 1–8. https://doi.org/10.1007/s42452-019-1849-6
23. A. Saiyathibrahim, S. Seenivasan, R. Premkumar, and D.G. Mohan, Multi-response Optimization of Wire EDM Parameters for AISI 304 SS Using Grey Relational Analysis, *J. Inst. Eng. India Ser. D*, 2025 https://doi.org/10.1007/s40033-025-00882-1
24. M.K. Sinha, S. Ghosh, and V.R. Paruchuri, Modelling of Specific Grinding Energy for Inconel 718 Superalloy, *Proc. Inst. Mech. Eng. Part B J. Eng. Manuf.*, 2019, **233**(2), p 443–460. https://doi.org/10.1177/0954405417741513
25. P. Mandal, S. Mondal, R. Cep, and R.K. Ghadai, Multi-objective Optimization of an EDM Process for Monel K-500 Alloy Using Response Surface Methodology-Multi-Objective Dragonfly Algorithm, *Sci. Rep.*, 2024, **14**(1), p 20757. https://doi.org/10.1038/s41598-024-71697-5
26. E. Kilickap, A. Yardimeden, and Y. Hışman Çelik, Mathematical Modelling and Optimization of Cutting Force, Tool Wear and Surface Roughness by Using Artificial Neural Network and Response Surface Methodology in Milling of Ti-6242S, *Appl. Sci.*, 2017, **7**(10), p 1064. https://doi.org/10.3390/app7101064
27. R. Świercz, D. Oniszczuk-Świercz, and T. Chmielewski, Multi-response Optimization of Electrical Discharge Machining Using the Desirability Function, *Micromachines*, 2019, **10**(1), p 72. https://doi.org/10.3390/mi10010072
28. S. Gopalakannan and T. Senthilvelan, Optimization of Machining Parameters for EDM Operations Based on Central Composite Design and Desirability Approach, *J. Mech. Sci. Technol.*, 2014, **28**, p 1045–1053. https://doi.org/10.1007/s12206-013-1180-x
29. L. Kumar, A. Goyal, S. Garg, and R.K. Phanden, Predictive Modeling of Drilling Machine Performance for Jute Fiber-Reinforced Polymer Composites Using GA, TLBO, and GRA-Based RSM Approaches, *Int. J. Interact. Des. Manuf.*, 2025, **19**(3), p 2265–2281. https://doi.org/10.1007/s12008-024-01892-1
30. M. Manjaiah, R.F. Laubscher, A. Kumar, and S. Basavarajappa, Parametric Optimization of MRR and Surface Roughness in Wire Electro Discharge Machining (WEDM) of D2 Steel Using Taguchi-Based Utility Approach, *Int. J. Mech. Mater. Eng.*, 2016, **11**, p 1–9. https://doi.org/10.1186/s40712-016-0060-4
31. R. Kesavalu and M. Subramanian, Comprehensive Analysis and Optimization of Wire-Cut EDM Process Parameters for Improved Surface Integrity and Material Removal Rate in Duplex Stainless Steel, *Matéria (Rio de Janeiro)*, 2024, **29**(4), e20240692. https://doi.org/10.1590/1517-7076-RMAT-2024-0692
32. J.A. Abbasi, M. Jahanzaib, M. Azam, S. Hussain, A. Wasim, and M. Abbas, Effects of Wire-Cut EDM Process Parameters on Surface Roughness of HSLA Steel, *Int. J. Adv. Manuf. Technol.*, 2017, **91**, p 1867–1878. https://doi.org/10.1007/s00170-016-9881-9
33. B. Choudhuri, R. Sen, S.K. Ghosh, and S.C. Saha, Comparative Machinability Characterization of Wire Electrical Discharge Machining on Different Specialized AISI Steels, *Bull. Mater. Sci.*, 2020, **43**, p 1–12. https://doi.org/10.1007/s12034-019-1982-2
34. A. Mandal and A.R. Dixit, State of Art in Wire Electrical Discharge Machining Process and Performance, *Int. J. Mach. Mach. Mater.*, 2014, **16**(1), p 1–21. https://doi.org/10.1504/IJMMM.2014.063918
35. Y. Nawaz, S. Maqsood, K. Naeem, R. Nawaz, M. Omair, and T. Habib, Parametric Optimization of Material Removal Rate, Surface Roughness, and Kerf Width in High-Speed Wire Electric Discharge Machining (HS-WEDM) of DC53 Die Steel, *Int. J. Adv. Manuf. Technol.*, 2020, **107**, p 3231–3245. https://doi.org/10.1007/s00170-020-05175-3
36. C.A. Huang, F.Y. Hsu, and S.J. Yao, Microstructure Analysis of the Martensitic Stainless Steel Surface Fine-Cut by the Wire Electrode Discharge Machining (WEDM), *Mater. Sci. Eng. A*, 2004, **371**(1–2), p 119–126. https://doi.org/10.1016/j.msea.2003.10.277
37. S. Zahoor, H.A. Azam, M.P. Mughal, N. Ahmed, M. Rehman, and A. Hussain, WEDM of Complex Profile of IN718: Multi-Objective GA-Based Optimization of Surface Roughness, Dimensional Deviation, and Cutting Speed, *Int. J. Adv. Manuf. Technol.*, 2021, **114**, p 2289–2307. https://doi.org/10.1007/s00170-021-06916-8
38. K. Lal and R. Trehan, Recent Progress in Surface Integrity for Wire Electrical Discharge Machining of Inconel Alloys, *Adv. Mater. Process. Technol.*, 2025 https://doi.org/10.1080/2374068X.2025.2484235